DATA FUSION USING WAVELET PACKET AND WAVELET FRAME TRANSFORM TO IMPROVE THE SEGMENTATION RESULTS OF MRI SKULL IMAGES

Researcher:
Baqir Ali
REG NO. 180-FET/MSEE/F08

Supervisor:
Dr. Hammad A. Qureshi
Co-Supervisor:
Dr. Ihsan-ul-haq

Department of Electronic Engineering

Faculty of Engineering and Technology

International Islamic University, Islamabad

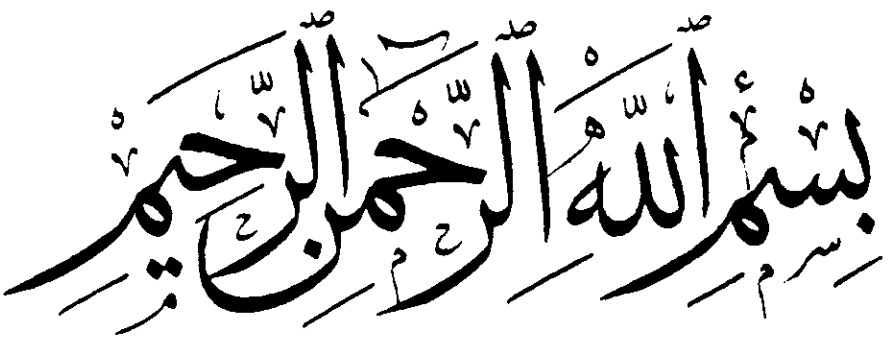
بسم الله الرحمن الرحيم

Dedicated to my dear father and mother

(Acceptance by the Viva Voce Committee)

Title of thesis Data fusion using Wavelet Packet and Wavelet Frame Transform to Improve the segmentation results of MRI skull images

Name of student Baqir Ali

Registration NO 180-FET-MSEE-F08

Accepted by the Department of Electronic Engineering INTERNATIONAL ISLAMIC UNIVERSITY, ISLAMABAD, in partial fulfillment of the requirements for the Master of Philosophy Degree in Electronic Engineering with specialization in Image Processing.

Viva voce committee

Dean
Dr. Ghulam Yasin Chohan
FET

Chairman
Dr. Muhammad Zubair
DEE, FET

External Examiner
Dr. H.M. Faisal Zafar
S.S. KRL

Internal Examiner
Professor Dr. I.M. Qureshi
DEE, FET

Supervisor
Dr. Hammad A. Qureshi
Assistant Professor, NUST

Co-supervisor
Dr. Ihsan-ul-Haq
Assistant Professor, FET

Day, month, year

ABSTRACT

In the last two decades computer vision based medical image analysis has become very popular. In the field of medical diagnosis image processing is used for different applications. The driving push behind this change is digitization of media and the increased processing power of the computing machine. The medical images are mostly obtained for diagnosis of internal diseases and sometimes also for external diseases. There are different techniques which are used to attain images of internal aspects of the human body. MRI images are used for disease analysis and better visualization of the human brain. In our work, we use Discrete Wavelet Packet Frames (DWPF) for the selection of useful image representations (WPFs) which are further fused together and used for K-means clustering. We compare our results with K-means clustering results of raw data.

In first step DWPF in applied for decomposition up to three levels. Then based upon entropy and energy values of each frame we select the most useful WPFs for further processing. These selected WPFs are normalized using min-max normalization. Later on K-means clustering is applied after fusion of these selected WPFs. We change the input parameters of K-means clustering such as number of clusters (K) and distance functions for obtaining better results.

Our technique provides improved segmentation results using K-means clustering over DWPF frames. We also compare our results with K-mean clustering on raw image data and show that our results are much improved for lower value of K.

ACKNOWLEDGEMENT

First of all I would like to thanks my supervisor Dr. HAMMAD A. QURESHI with the help of him this thesis could be possible. I cannot express in words about the guidance he provided me during my research.

I would also like to thanks faculty of engineering and technology, International Islamic university and School of Electrical Engineering and Computer Science (SEECS), National University of Science and Technology (NUST) specially graphics and visual computing lab of SEECS, where I worked for my thesis. I would also like to thanks Dr. IHSAN-UL-HAQ, my brothers, my sister and my parents for their affection and prayers.

TABLE OF CONTENTS

LIST OF TABLES

LIST OF FIGURES

(To be submitted to the department at the time of submission of Thesis by the supervisor)

FORWARDING SHEET

The thesis entitled Data fusion using Wavelet Packet and Wavelet Frame Transform to Improve the segmentation results of MRI skull images submitted by Baqir Ali in partial fulfillment of MS degree in Electronic Engineering with specialization in Image Processing has been completed under my guidance and supervision. I am satisfied with the quality of student's research work and allow him to submit this thesis for further process of as per IIU rules & regulations.

Date: 03-08-2012

Signature:

Name: Dr. Hammad A. Qureshi

CHAPTER # 1
INTRODUCTION

1.1. Introduction

In last two decades computer vision based image analysis has become very popular. In the field of medical diagnosis image processing is used for different applications. The driving push behind this change is digitization of media and the increased processing power of the computing machine. The medical images are mostly obtained for diagnosing internal diseases and sometimes also for external diseases. There are different techniques which are used to attain images of internal aspects of the human body; some of them are mentioned in Chapter 2. The task of detecting diseases has been largely viewed as a medical image segmentation problem.

1.2. Image segmentation

Image segmentation is the concept used to extract some useful information from an image. This information is used for different purposes i.e. in the field of medical imaging the extracted data is used for better visualization of diseased area. There are different techniques which are used for segmentation such as thresholding [1], region growing, watershed [2, 3] edge detection[2, 6, 7], template matching, K-mean clustering[3, 8], markov random fields [1] etc. These techniques are suitable for different types of data-sets or images. In these techniques, i focus on some region of interest for example diseased area (tumor or enhanced tissues) in medical science. To understand the concept of segmentation, some segmented images are shown in Figure 1 as

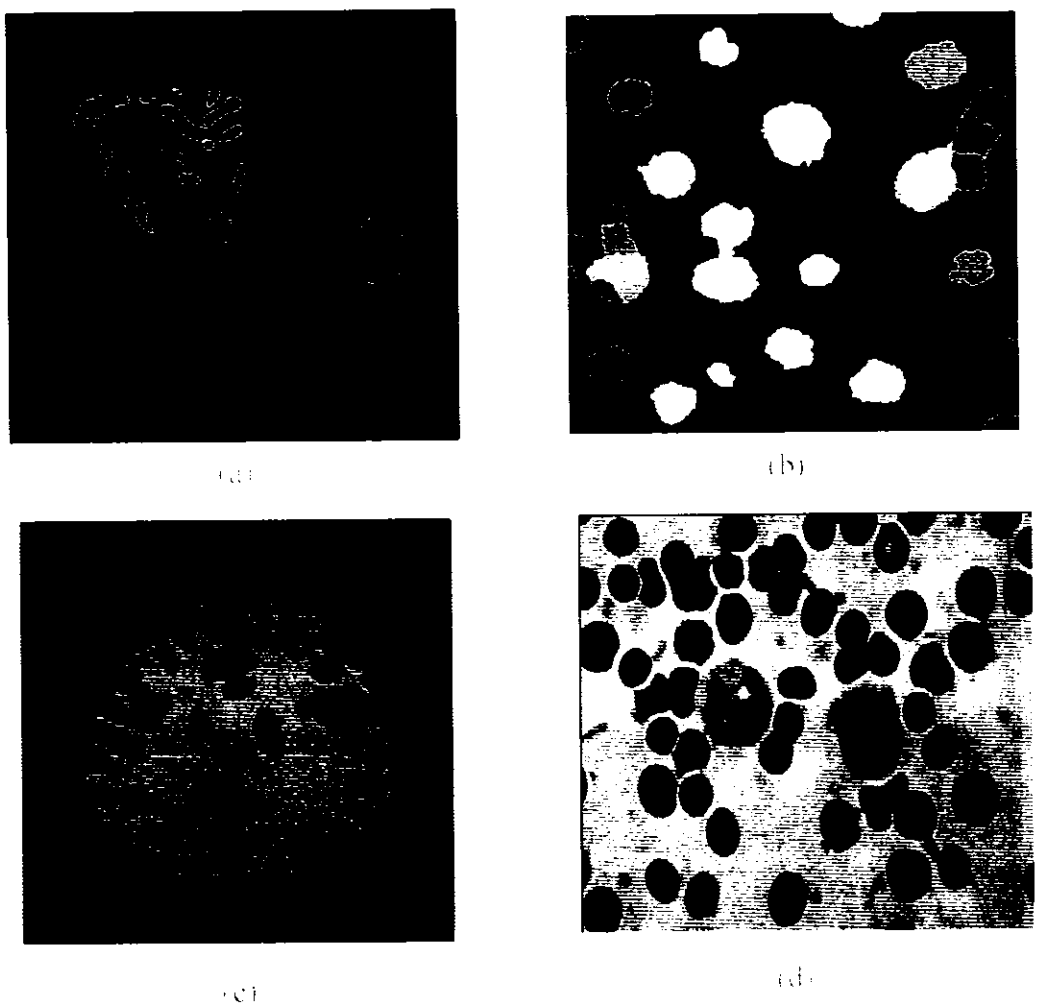

(a) (b)

(c) (d)

Figure1. The (a) and (d) shows the segmentation of different blood cells. (b) Shows the simple concept of object segmentation. (c) shows the segmentation of human brain

I work on MRI images of human brain and segment anomalies in brain. MRI can detect variety of conditions of the brain such as tumors, bleeding, swelling, structural abnormalities and problems with the blood vessels. In case of brain images doctors are

interested in the tumor or enhanced mass of brain tissue. Sometimes the information about the gray and white matter is also needed.

1.3. Disease Detection

For any doctor the most important feature in a medical image is the diseased area. In the field of medical imaging there are different types of diseases that can be segmented. The diseases may be internal or external. The images of diseases are mostly taken for internal disease like broken boon, internal tumor or other internal diseases. Some of them are shown in Figure2

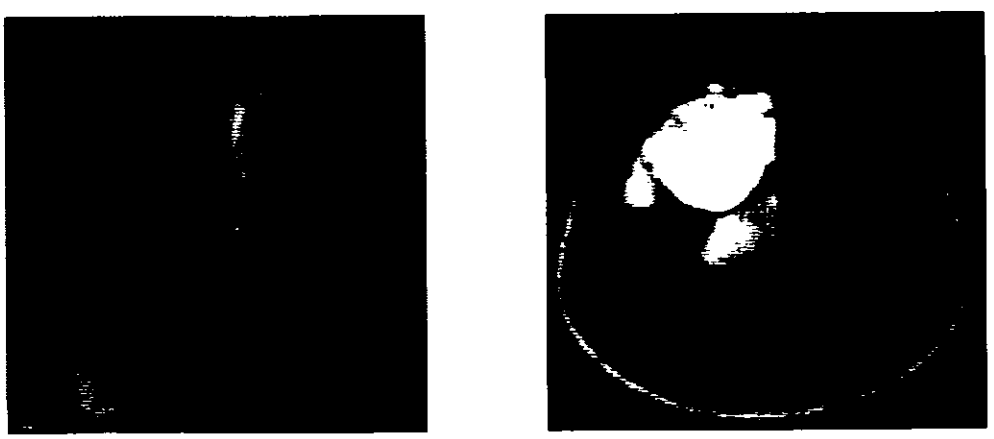

(a) (b)

Figure 2 The portion shows the broken bone of human and (b) shows some diseased area in MRI image of human brain

1.4. Defect or Disease detection Approaches

- Statistical Approaches
- Structural Approaches

- Spectral Approaches

1.5. Problem statement and proposed method

I need a method which has joint localization in space and time (spatiotemporal). The wavelets transform deals with both i.e. frequency and time domain. So the wavelet transform is one of the best methods used for analysis of medical images. The discrete wavelet transform captures both frequency and location information (location in time). In discrete wavelet transform after decomposition the resolution of each subband becomes different from original image. To overcome this problem the Discrete Wavelet Frame Transform (DWFT) is introduced which keeps the resolution of each subband the same after decomposition. In my proposed technique, I also decompose the detailed subbands after first step of decomposition; due to this property I can call my technique Discrete Wavelet Packet Frame (DWPF). It is popularly believed that K-means clustering can only converge to local minimum, even though recent research has shown with large probability that K-means could converge to the global optimum specially when clusters are well separated [4, 5]. After the selection of useful Wavelet Packet Frames (WPFs) I perform K-means clustering for disease segmentation. These WPFs are not ever used in K-means clustering. So it's a novel approach to segment the brain diseases using WPFs. It's also important to describe that i change the distance functions in K-means clustering i.e. squared Euclidean distance function and city block distance function. Writer also takes account of the brain detailed information known as grey and white matter structure. The brain magnetic resonance imaging (MRI) as shown in Figure 2 (b) would not

highlight exact area of disease without using contrast enhancement. I can help the doctors to obtain better visualization of MRI data without using expensive contrast reagents (CRs). At the end i justify this proposed technique by comparing my results with simple K-mean clustering results. I use different values of K in K-means clustering. For better comparison i also use different distance function in K-means clustering and analyze the improvement in results of my proposed technique.

1.6. Thesis Objective

Medical images are used largely for disease analysis. Different techniques have also been adopted for disease detection. My objective in this thesis is to detect the abnormal part in the medical image using Discrete Wavelet Packet Frame with K-mean clustering to help the doctors in better analysis of disease. For obtaining MRI of human skull different types of expensive contrast agents are used. These types of medicines have their after side effects. Commonly used compounds for contrast enhancement are Gadolinium (III) based. This Gadolinium (III) contrast agents are frequently used for brain tumor MRI contrast enhancement [9]. I may be able to reduce the cost of MRI. My main thesis objective is to obtain the better contrast images containing detailed information about the diseased area as well as surrounding information of diseased area to help in better visualization and analysis and diagnosis of disease by the doctor.

1.7. Thesis Organization

In Chapter 2, i will discuss wavelets, application of wavelet transform, and present a review of Magnetic Resonance Imaging (MRI). Second chapter also contains description

of common data Fusion methods. At the end of second chapter some disease or defect detection approaches are also discussed. In Chapter 3 i describe the comprehensive detail of my proposed technique and complete method for selection of useful Wavelet Packet Frames (WPF). In Chapter 4 all the results and their comparison is made with a discussion about how my results are better as compared to simple K-means clustering. At the end in Chapter 5, i will provide conclusions as per the results along with the possibility of future work in this field.

CHAPTER # 2

LETERATURE REVIEW

Different techniques used for disease detections in medical images are discussed in this chapter. First approach is statistical approach comprises of gray level co-occurrence matrices, local binary pattern, cross correlation, auto correlation, edge detection techniques etc. Second approach is structural approach. Third approach is Spectral Approaches . More details of these approaches are given below.

2.1. Wavelet Transform and Medical Imaging

The time and frequency resolution problem is because of a physical phenomenon (Heisenberg's Uncertainty Principle) and survive regardless of which transform is used. It is probable to analyze a signal with the use of an alternate technique called wavelet transform (WT). The wavelet transform analyses the signals of diverse frequencies with diverse resolutions. The wavelet transform is used to provide fine time resolution and poor frequency resolution at very high frequencies and vice versa. This transform makes sense when signal has high frequency for small duration and low frequency for large durations. The review [10] shows, diverse use of wavelet transform in biomedical applications. The wavelet tools provide localization in time-frequency plane. This property of wavelet is the secret of its remarkable success in biomedical field. In conventional phase-encoded MRI, the Fourier basis functions are used that make the process very slow since the basis functions (sine and cosines) are delocalized spatially.

On the other side, wavelet basis are better localized spatially and possibly make the MRI process fast [10].

2.2. Applications of Wavelets Transform

Some basic applications (in which Discrete Wavelet Transform is used) are:

- Medical imaging,
- Astrophysics,
- Analyze clumping of galaxies to analyze structure at various scales,
- Analyze fractals, chaos,

Wavelet transforms are now being adopted for a vast number of applications, often replacing the conventional Fourier Transform [11]. Many areas of physics have seen this paradigm shift, including Turbulence and quantum mechanics. In computer vision and image processing, the notion of scale-space representation and Gaussian derivative operators is regarded as a canonical multi-scale representation. One use of wavelet approximation is in data compression. Like some other transforms, wavelet transforms can be used to transform data, and then encode the transformed data, resulting in effective compression.

2.3. Introduction of Medical Imaging

Number of methods can be used for disease detection in medical images. Some important techniques are gray level co-occurrence matrices, autocorrelation, thresholding , edge

detection [7], histogram [12], local binary pattern [12], bi level thresholding [1, 12], Fourier transform, short time Fourier transform, discrete wavelet transform and Discrete Wavelet Frame Transform. The technique like bi level thresholding is good only for high contrast images [12, 13]. Local binary patterns have been reported to provide lower performance than gray level co-occurrence matrix. The histograms are invariant to translation and rotation. Histogram level ranges from 0 to 255 for 8 bit images. Edge detection is suitable only for plane images with low resolution [12]. Discrete Fourier transforms only deal in frequency domain but not in time domain. Now a day diagnostic imaging is a useful tool in medicine. Different methods are used in medical imaging for further analysis of disease i.e. magnetic resonance imaging (MRI). Segmentation techniques vary widely and are used according to the specific application, imaging modality and some other factors. For example, the segmentation of liver tissue has different requirements from the segmentation of the brain tissue. In medical field, an image is a compilation of measurements or image intensities in two-dimensional (2-D) or three-dimensional (3-D) space. If the image is made by more than one measurement then the image is called multichannel image or a vector image. In MRI the images are acquired in discrete space.

2.4. Magnetic Resonance Imaging (MRI)

The majority of doctors use MRI images for medical image analysis, especially in brain imaging. Frequent use of MRI images of brain is because of MRI's ability to give a compilation of high resolution (1mm cubic voxels), a high signal to noise ratio and

excellent soft tissue contrast. The tissue of different body parts having different compositions is the reason why they are viewed at different contrast levels. Direct comparisons of different techniques for MRI images segmenting are available [14, 15, 16] because of its capability to vary contrast using number of tissue parameters and many different extra sequences exist for acquiring MRI images. The set of suitable contrasts can be used for every appropriate tissue [18]. Furthermore, due to the anatomical and physiological inconsistency between subjects, different populations may involve different extra sequences [19]. The literature on segmentation in MRI specifically focuses on the segmentation of human skull scan. Different three general goals [1] in this application are:

1) Segment brain tissue into gray matter, cerebrospinal fluid and white matter

2) Extract brain volume

3) Delineate specific brain structure such as the hippocampus

The machine used for MRI is referred in Figure 3.

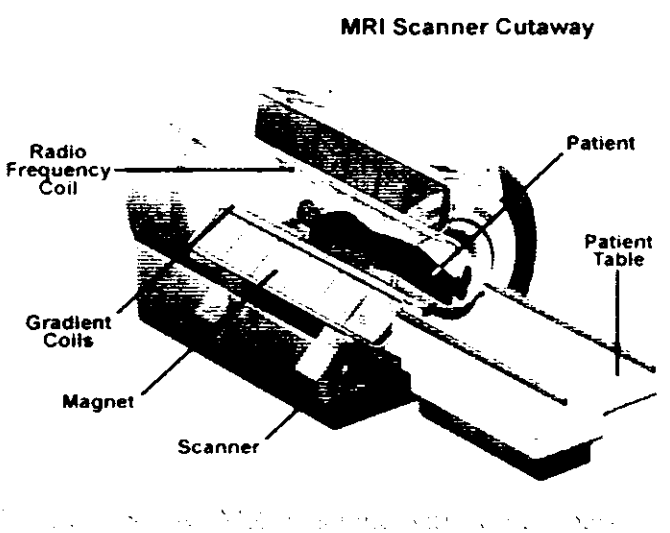

Methods that challenge to segment brain tissue as cerebrospinal fluid, gray matter and white matter use either T1-weighted scalar data [17, 20, 21, 22, 23, 24] or multispectral data [25, 26, 27, 28, 29, 30, 31, 32, 33, 34]. One major complexity in the segmentation of MRI images is known as intensity inhomogeneity artifact [35, 36, 37]. This issue causes a shading effect to appear on the image. The shading effect creates difficulties for the diagnosis of exact diseased area especially in the case of human brain analysis. The captivating feature of MRI images is its varying contrast characteristic. Different intensity and gray level contrasts are obtained according to the situation of patient.

2.5. Image Fusion

In the process of image fusion two or more images are combined into a single image holding important features from the original image. There are many important applications of image fusion that include medical imaging, remote sensing, microscopic imaging, robotics and computer vision.

2.6. Common data fusion methods

- Intensity hue saturation (HIS) transform [38]
- Principal component analysis (PCA) [39]
- Discrete wavelet transform (DWT) [40]

2.6.1. Intensity Hue Saturation (HIS) Transform

Intensity hue saturation (IHS) is commonly used fusion method for the remote sensing data. In this method the three basic image colors R, G, B are first converted into the HIS color space as [41].

$$\begin{pmatrix} I \\ V_1 \\ V_2 \end{pmatrix} = \begin{pmatrix} \frac{1}{3} & \frac{1}{3} & \frac{1}{3} \\ \frac{1}{\sqrt{6}} & \frac{1}{\sqrt{6}} & \frac{-2}{\sqrt{6}} \\ \frac{1}{\sqrt{2}} & \frac{-1}{\sqrt{2}} & 0 \end{pmatrix} \begin{pmatrix} R \\ G \\ B \end{pmatrix} \quad (1)$$

$$H = \tan^{-1}\left(\frac{V_2}{V_1}\right) \quad (2)$$

$$S = \sqrt{V_1^2 + V_2^2} \quad (3)$$

In HIS, I represent intensity, H represents hue and S represents saturation. In the above equations (Eq1, Eq2 and Eq3) V1 and V2 are the intermediate variables. Fusion profits by replacing I with panchromatic image information of high resolution. The resultant fused image is obtained by taking inverse transformation from HIS to RGB space as mentioned in Equation (4).

$$\begin{pmatrix} R \\ G \\ B \end{pmatrix} = \begin{pmatrix} 1 & \frac{1}{\sqrt{6}} & \frac{1}{\sqrt{2}} \\ 1 & \frac{1}{\sqrt{6}} & \frac{-1}{2} \\ 1 & \frac{-2}{\sqrt{6}} & 0 \end{pmatrix} \begin{pmatrix} I \\ V_1 \\ V_2 \end{pmatrix} \quad (4)$$

2.6.2. Principal component analysis (PCA)

Principal component analysis (PCA) is one of the general statistical methods that transform multivariate information with correlated variables into one with uncorrelated variables. The resultant variables are received as the linear combination of real variables. This method has been commonly used in image data compression, image enhancement, image encoding and image fusion.

2.6.3. Discrete wavelet transforms (DWT)

In the DWT, a signal is decomposed in to a multiresolution decomposition which has both low frequency and high frequency information. For the fusion, the source image is geometrically registered and also decomposed at the same resolution. Inverse wavelet transform is performed to obtain fused image. The result of the fusion does not change the radiometry of the real image [42].

2.7. Defect or disease detection Approaches:

2.7.1. Statistical Approaches

Gray level co occurrence matrices: The approach gray level co-occurrence matrices (GLCM) some time also known as spatial gray level dependence method. This method is frequently used for the analysis of texture features and medical image features. With the help of this GLCM image features like entropy of the image, energy of the image and contrast of the image can be calculated [13]. The basic idea behind this technique is repetitive incidence of some gray levels in the one image. This GLCM method can also

face some problems [13]. In this method there is no received solution for calculating the best displacement vector. To get rid of this issue the number of gray levels must be reduced. So the size and shape of the matrix become also controllable.

Autocorrelation: This approach is mostly useful in the case where the textures having the nature of repetition, like in wood, marble and some medical images. This method examines the relation of the image with itself and image which is translated with the displacement vector [13].

Local binary pattern: The contrast of the local image can be determined with the help of local binary pattern (LBP) method. In this LBP method the value of the centered pixel of sliding window is used as threshold value for its surrounding neighborhood pixels [12]. So by changing the gray level at the center of sliding window thresholding value can be changed.

Bi-level Thresholding: In the case of high contrast defects the gray level thresholding is mostly used. The technique called bi level thresholding provides good results as compared to other defect detection techniques [13]. This technique has a very useful and complex pattern [12].

Cross correlation: Cross correlation method is used for comparing features between two images. This is a very precise and direct method for measuring similarities of two images [13]. Changing level value identifies the defect in the resultant image. The mathematical form of this method is represented by Equation 5 as

$$(f * g)(t) = \int_{-\infty}^{\infty} f^*(\tau) g(t+\tau) d\tau \tag{5}$$

In the above Equation 5 f^* is complex conjugate of f. The discrete form of this method can be represented by Equation 6 as

$$(f*g)[n]=\sum_{m=-\infty}^{\infty} f^*[m]g[n+m] \tag{6}$$

Edge detection: In an image sudden change in pixel value create edges in the image. Some edges are narrow and some are wide. Two edge detection levels are used called micro level and macro level. The operators used for edge detection are sobel operator, canny operator, roberts operator and prewitt operator.

Micro edges: The narrow edges can be detected by using small edge operators. These edges are called sharp edges.

Macro edges: The macro edges can be detected by using large edge operators. These edges are known as wide edges.

Histogram: Defects can be highlighted with the help of histograms as well. Different other parameters are involved for the sake of histogram equalization. These parameters are mean of histogram, standard deviation, median and variance.

2.7.2. Structural Approaches

In the field of medical image analysis for responsibilities like locating diagnostically valuable areas, structural approaches have been widely used [43], penetrating between normal and cancerous tissues [44] and separating tumours of various grades [45]. These types of techniques have also been used in finding unusual tissue regions in colorectal

histology [43, 44]. With the use of fractal geometry nuclear dimensions have been studied [46].

2.7.3. Spectral Approaches

In the field of computer vision the spectral approaches are very useful. This approach is not appropriate for the random texture materials [12].

Fourier transform: Fourier transform is commonly used for global defects. This technique is good only for frequency domain. The local and small defects detections cannot be performed by ordinary Fourier transform exactly. For large data sets the Fourier transform become very complex and time consuming [12].

Windowed Fourier transform: The Fourier transform and discrete Fourier transform are good only for frequency domain. There is a need of such technique which deals with both frequency and time domain. So with the help of this windowed function the local defects can also be analyzed. This also has limitations.

Wavelet transform: Wavelet transform involves multiresolution decomposition. This feature attracts the attention of most of the researchers for the extraction of image features. With the help of wavelet transform one image can be decomposed into different subbands. So the detailed characteristics of the image can be analyzed [12].

CHAPTER # 3

METHODOLOGY AND TECHNIQUES

In this study I intend to develop technique for better visualization and segmentation of brain tissue in medical images. The detail of proposed method is discussed in this chapter. The study was carried out in collaboration with Pakistan Institute of Medical Sciences (PIMS).

3.1 Data

Magnetic Resonance Imaging (MRI) based images of the human brain were collected from PIMS hospital Islamabad. Some of these were selected for analysis. All these MRI images are real images of different patients with brain diseases in different parts of the brain. These MRI images of human brain have been collected with the permission of PIMS hospital doctors and patients. The diseases incurred or seen in my data set includes tumor, presence of air ball and water ball etc. Some of the images acquired are given in Figure 4.

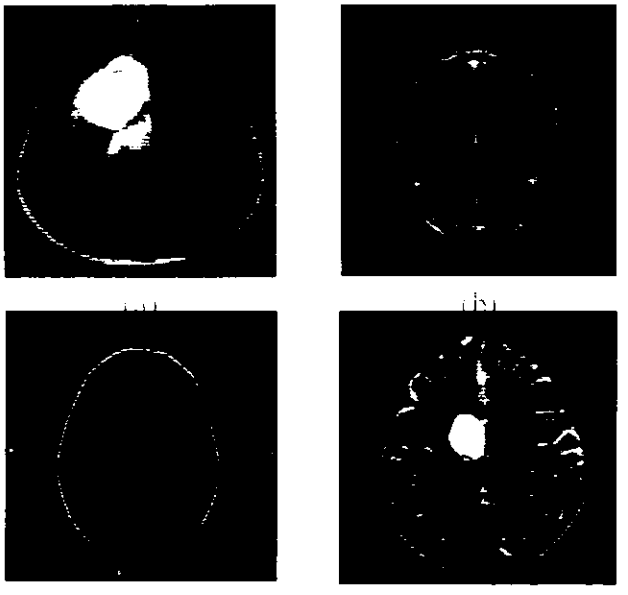

3.2 Wavelets

I have used un-decimated wavelet packet transform which is referred to as wavelet frames for simple wavelet transform however for wavelet packets i will refer to it as wavelet packet frames. The difference between my approach and classic wavelet frames is that i decompose high frequency subbands as well (as carried out in wavelet packets). A brief description of the technique along with related concepts is given next.

3.2.1. Discrete Wavelet Transform (DWT)

If i have discrete function defined as f(n) then the definition of discrete wavelet transform (DWT) is given by Equation 7.

$$C(a,b)=C(j,k)=\sum_{n\in Z} f(n)\psi_{j,k}(n) \tag{7}$$

In Equation 7 value of j controls the dilation and the value of k represents the translation. If the parameters a, b are defined in this way that $a=2^j$, $b=2^jk$, the analysis is referred to as dyadic [47]. A wavelet function is defined by Equation 8.

$$\psi_{j,k}(n)=2^{-j/2}\psi(2^{-j}n-k) \tag{8}$$

3.2.2.Two dimensional Discrete Wavelet Transform (2-D DWT)

Digital images require a two dimensional wavelet transform. The 2-D DWT analyzes the images across rows and columns in progression so as to break up vertical, horizontal and

diagonal details in three high frequency subbands. In the result of 2-D discrete wavelet transform four different subbands are formed. The one level 2-D Wavelet transform is represented by Figure 5.

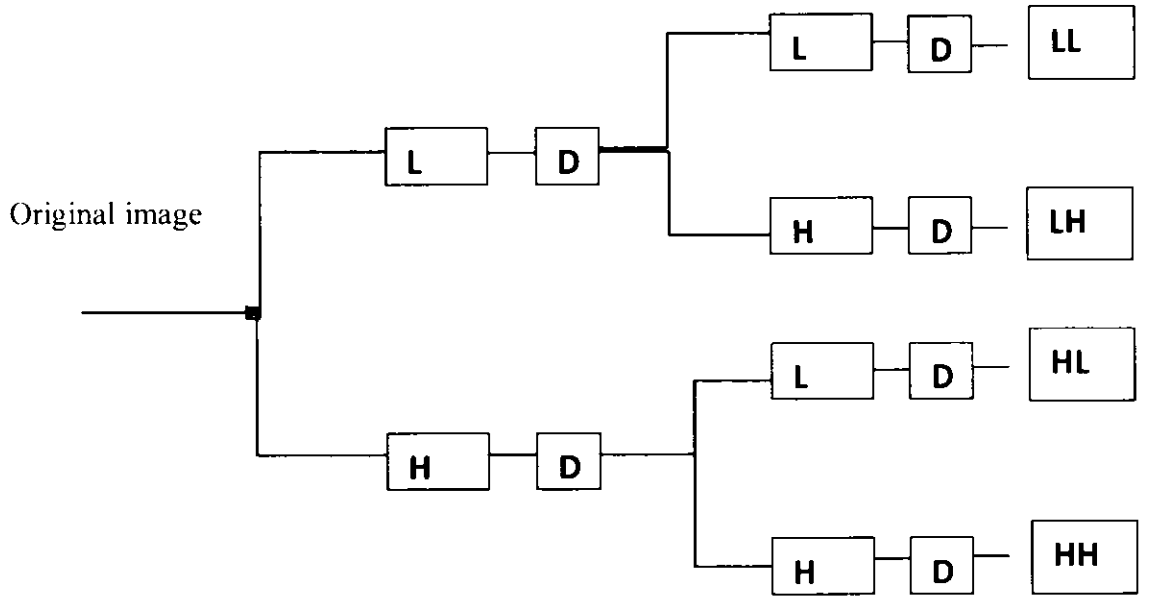

Figure 5: One level Decomposition of 2-D Discrete Wavelet Transform (DWT)

In the above diagram **L** represents the low pass filter, **H** is the high pass filter and **D** represents down sampling by 2 used in dyadic decomposition. So the four resultant subbands are LL, LH, HL and HH as demonstrated in Figure 5.

- LL shows the low pass approximation of original image
- LH shows the detailed horizontal subband
- HL shows the detailed vertical subband
- HH shows the detailed diagonal subband

3.2.3. Discrete Wavelet Frame Transform in Two Dimensions (2-D DWFT)

In the ordinary discrete wavelet transform the size of the approximation band and all the three detailed subbands are different from original image where as in discrete wavelet frame transform all the subbands are of the same size as original image. In the two dimensional discrete wavelet transform there is a factor called down sampling factor due to which the size of the subbands becomes different from the original image. This difference is illustrated in Figure 6.

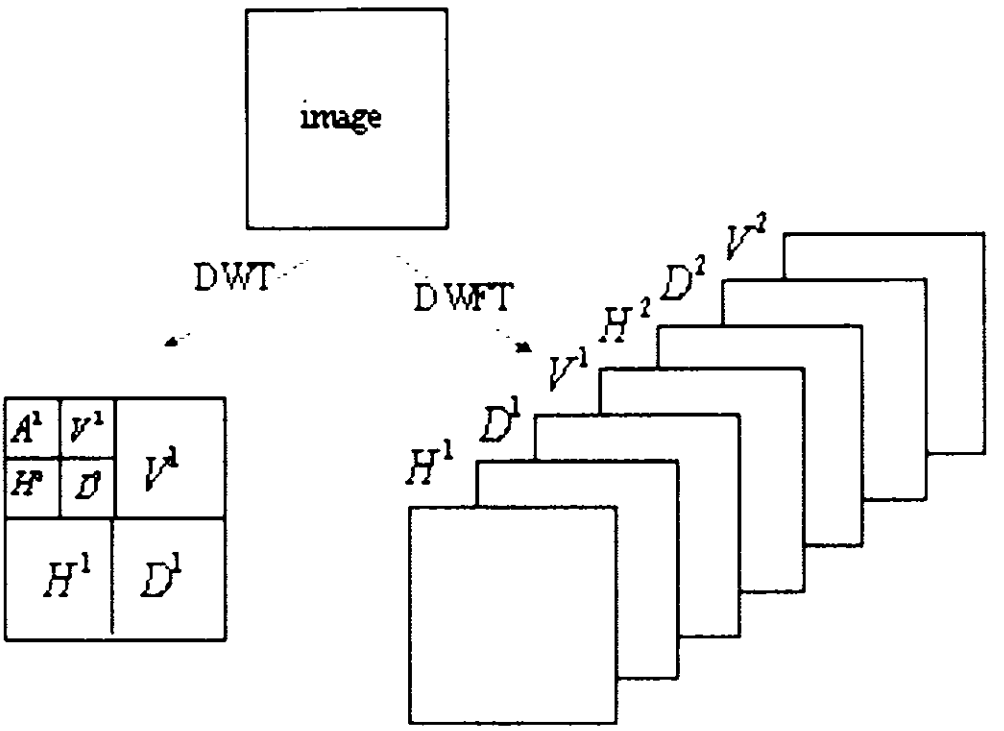

Figure 6 The difference between Discrete Wavelet Transform (DWT) and Discrete Wavelet Frame Transform (DWFT)

From the Figure 6 the difference between DWT and DWFT is quite clear. After the decomposition using DWT the subbands are of different size as compared to the original image. In the decomposition using DWFT all the subbands are of the same size as the original image. For example if the size of original image is 256x256 then after the decomposition using Discrete Wavelet Frame Transform (DWFT) the four subbands are formed, the size each of subband is 256x256.

3.3. Introduction to Wavelet Families

Different families of wavelet are developed. Some especially useful families of wavelets are: Haar, Daubechies, Biorthogonal, Coiflets, Symlets, Morlet, Mexican Hat. Some other wavelets are Biorthogonal, Reverse Biorthogonal and Gaussian derivatives family etc.

3.4. Discrete Wavelet Packet Frame (DWPF)

In the proposed method, i take Discrete Wavelet Packet Frame (DWPF) of up to three steps and then select the useful subbands according to a selection criterion. These subbands are now referred as Wavelet Packet Frames (WPFs). The detail of the selection criteria is described in section 3.5. After the three steps of decomposition, a total of 52 WPFs are formed. The formation of the frames is given in Figure 7 shown below:

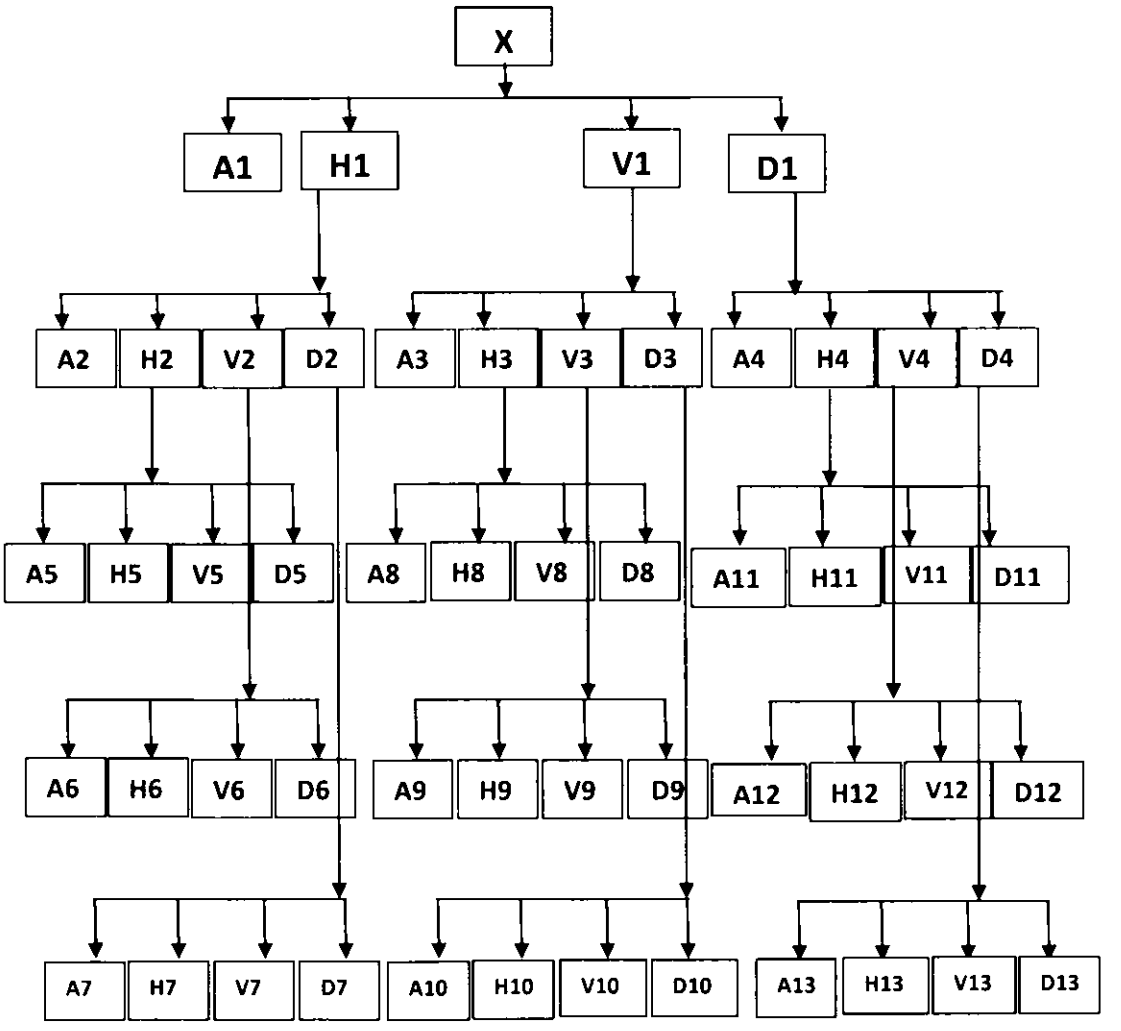

The above Figure 7 shows the subbands of Discrete Wavelet Packet Frame (DWPF) of up to three levels.

3.4.1. First level DWPF

In the first level DWPF the resultant wavelet packet frames (WPFs) are named as A1, H1, V1 and D1. In these resultant WPFs A1 represents the approximation subband, H1 represents the horizontal detail frame, V1 represents the vertical detail frame and D1 represents the diagonal detail frame. For further decomposition, the detailed information WPFs (H1, V1 and D1) are used. It must be noted here that the approximation frame is not decomposed as it is equivalent to the original image and decomposing it would produce WPFs equivalent to A1, H1, V1 and D1 and so on.

3.4.2. Second level DWPF

In the second level decomposition the resultant WPFs are as followed:

- From H1 further WPFs obtained are A2, H2, V2 and D2
- From V1 further WPFs obtained are A3, H3, V3 and D3
- From D1 further WPFs obtained are A4, H4, V4 and D4

So the total number of WPFs in this second level decomposition are A2, A3, A4 (approximation WPFs) and H2, H3, H4 (Horizontal WPFs), V2, V3, V4 (Vertical WPFs) and D2, D3, D4 (Diagonal WPFs).For the 3rd level decomposition i use only detailed WPFs of second level decomposition.

3.4.3. Third level DWPF

In the third level decomposition new resultant WPFs are as

- From H2 further WPFs are A5, H5, V5 and D5
- From V2 further WPFs are A6, H6, V6 and D6
- From D2 further WPFs are A7, H7, V7 and D7
- From H3 further WPFs are A8, H8, V8 and D8
- From V3 further WPFs are A9, H9, V9 and D9
- From D3 further WPFs are A10, H10, V10 and D10
- From H4 further WPFs are A11, H11, V11 and D11
- From V4 further WPFs are A12,H12,V12 and D12
- From D4 further WPFs are A13,H13,V13 and D13

These are new third level decomposition WPFs. In this third level decomposition the new approximation WPFs are A5, A6, A7, A8, A9, A10, A11, A12 and A13. The detailed WPFs in this third level decomposition are H5, H6, H7, H8, H9, H10, H11, H12, H13, V5 (Horizontal WPFs), V6, V7, V8, V9, V10, V11, V12, V13 (Vertical WPFs), D5, D6, D7, D8, D9, D10, D11, D12 and D13 (Diagonal WPFs). Hence, there are total 36 WPFs in this third level decomposition. It may be noted here that the number of WPFs at higher levels is rising exponentially. Some of these WPFs represent unique textural characteristics while the others represent redundant information. Figure 8 shows the vertical frame (V1, V9), horizontal frame (H1, H5) and diagonal frame (D1, D3). It can be seen from images in Figure 8 that there is considerable redundancy i.e. a lot of

similarity in the WPFs therefore i select only a subset of the overall frames for my analysis to reduce redundancy.

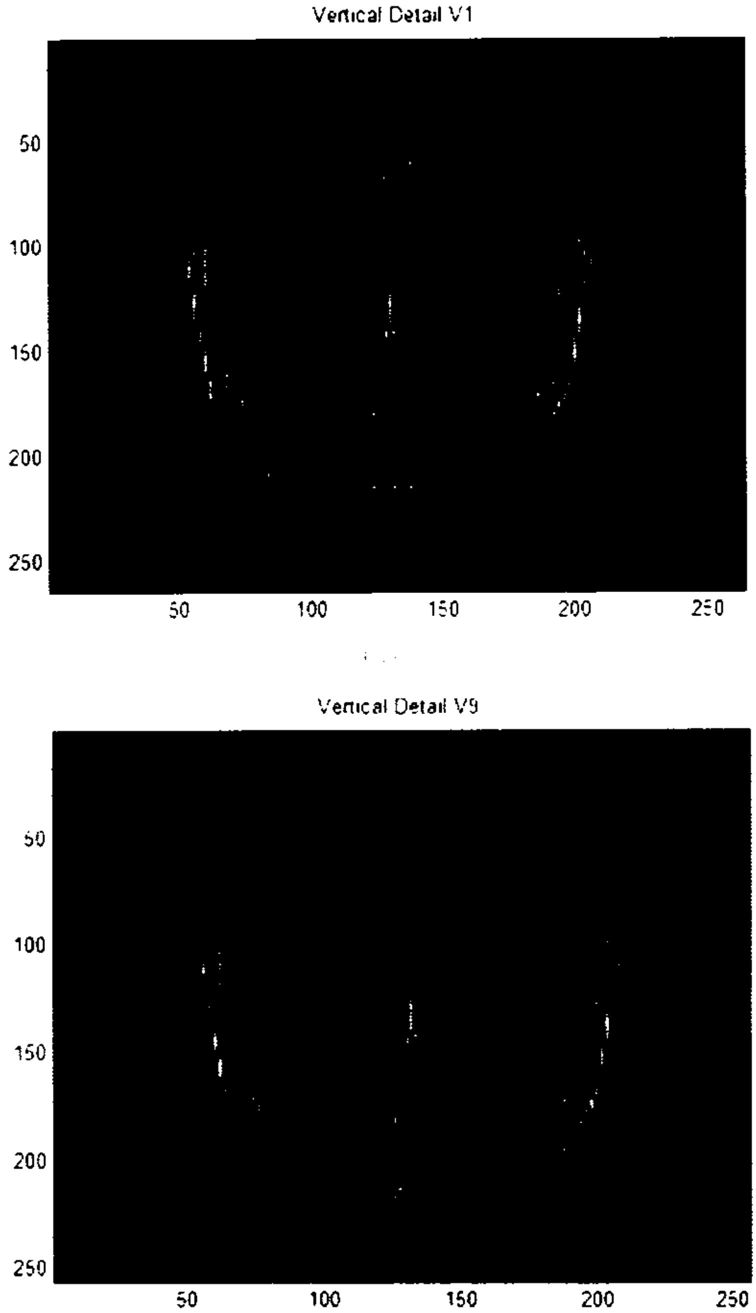

(b)

[illegible] Shows the vertical frame V[illegible] and [illegible] shows vertical [illegible] V9 (continued)

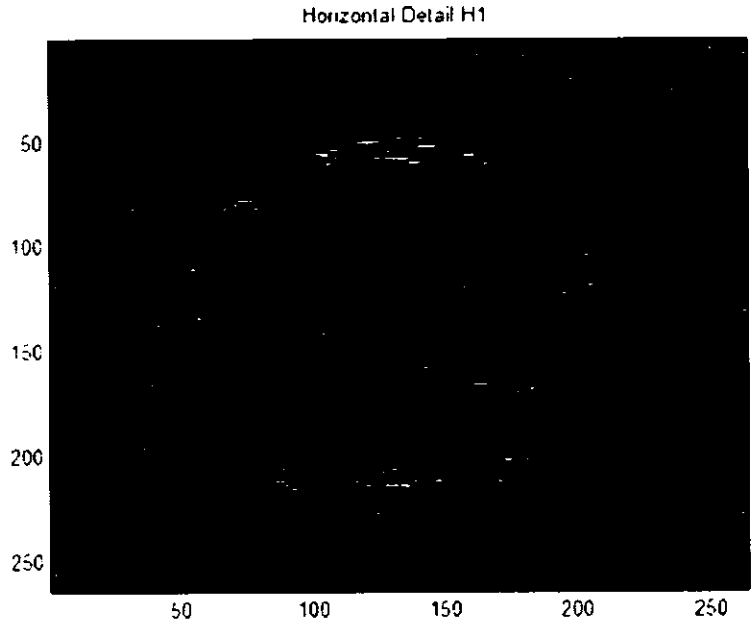

(c)

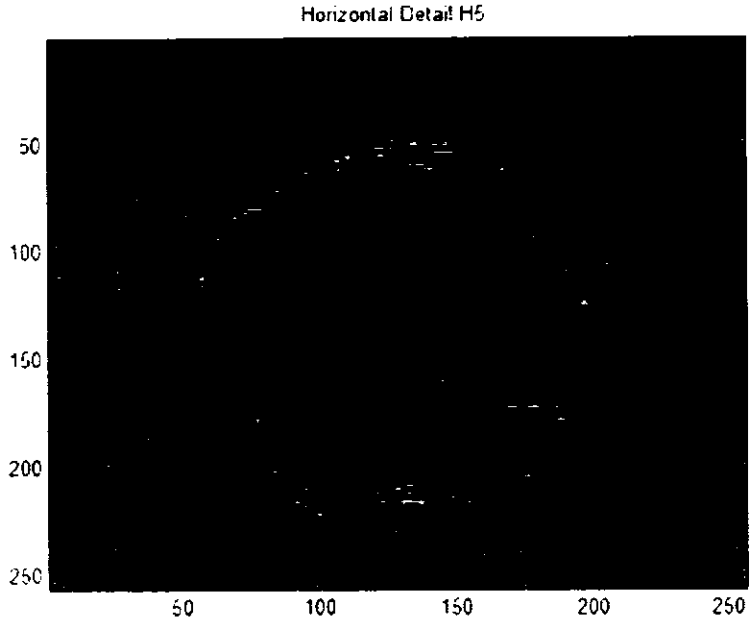

(d)

... (c) Shows the horizontal frame H1 and (d) shows horizontal ... H5 decomposed

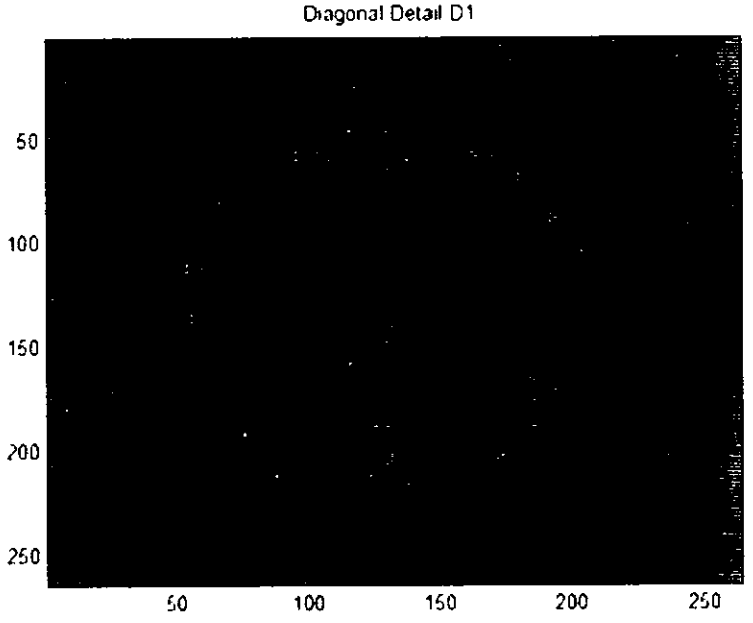

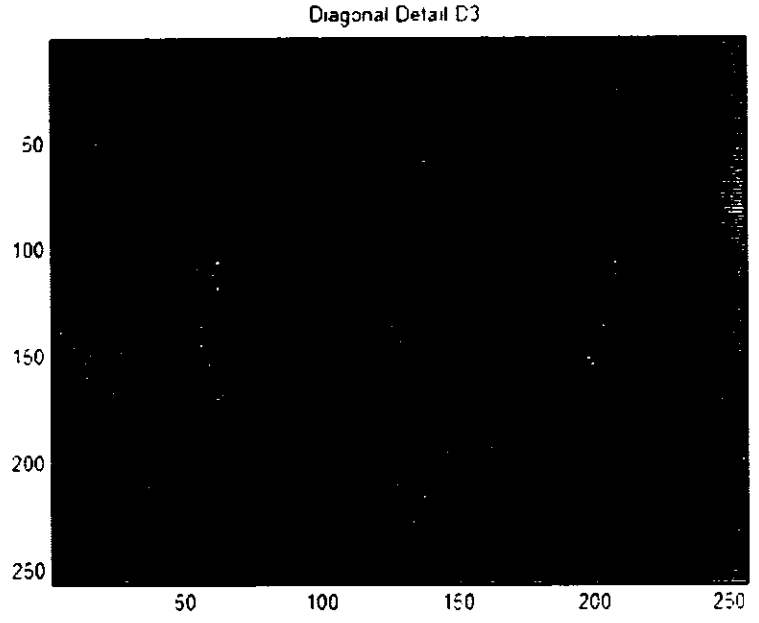

[illegible] shows diagonal detail D1 and (b) shows diagonal detail D3

3.5. Selection of useful WPFs

After decomposing all WPFs, my main focus is to select WPFs which have more useful textural information. The selection of useful WPFs helps us to acquire most relevant WPFs and also reduce redundancy in terms of features represented by each frame which leads to reduction in computation complexity. This step involves selecting useful WPFs as per the following criterion:

- Calculate the entropy of each frame
- Calculate the energy of each frame
- Arrange WPFs with decreasing entropy and energy value
- Select WPFs that are consistently valuable i.e. have high energy and entropy value for DWPF of various MRI images
- Selected WPFs are used for further analysis

3.5.1. Calculate the entropy of each frame

The entropy of a wavelet packet frame measures the amount of variation amongst the coefficients that exist in the frame. I prefer the higher values of entropy due to my interest in large variation as i intend to segment the MRI images i.e. anatomical structures from the background. The entropy of the frame is calculated using Equation 9.

$$Entropy(X) = -\sum_{i,j=0}^{N-1} x_{i,j} \log_2 x_{i,j} \tag{9}$$

Equation 9 gives us the entropy of each frame. After calculating the entropy of each frame the next step is to calculate the energy of each frame.

3.5.2. Calculate the energy of each frame

The energy of a wavelet frame shows the presence of valuable textural information. If there are more coefficients with non-zero values then the energy will be higher. I prefer WPFs having higher energy because they contain more information. The WPFs with lower energy values have less information about the original image. The energy of each frame is calculated with the help of following Equation 10.

$$Energy\ of\ X = \sum_{i=1}^{N} \sum_{j=1}^{N} (\left| x_{i,j}^{2} \right|) \tag{10}$$

In the above Equation 10, 'i' and 'j' represents the row number and column number respectively.

3.5.3. Arrange WPFs with decreasing entropy and energy value

For better selection of useful WPFs, the WPFs are re-arranged in decreasing order of entropy and energy values. The frames having higher entropy and energy value come first and the frame having lower entropy and energy value fall towards the end. The higher entropy and energy value wavelet packet frames (WPFs) are more useful than low entropy and low energy WPFs hence i need to set a criteria for the selection of WPFs. After this arrangement i proceed towards the selection of common high valued useful

frames i.e. frames found to be of high energy and high entropy in multiple DWPFs decomposition for different images.

3.5.4. Select WPFs that are consistently valuable

After the arrangement of all WPFs according to decreasing entropy and decreasing energy for various images in my data-set, i have useful WPFs at higher positions is the arrangement. So i select a limited number of WPFs i.e. top 10 WPFs for both entropy and energy values. These upper 10 WPFs have higher values for both entropy and energy. From these upper 10 WPFs, i select the common WPFs which are present in both entropy table and energy table. I also assign them numbering in descending order. For example i assign a number '10' to the frame having highest value. The frame at the second place is assigned a number '9', frame at third place is assigned a number '8' and so on up to tenth frame. These numbers are referred to as frame quality numbers.

Patient 1, Case 1 readings

Table 1: Entropy in decreasing order along with respective frame for patient 1 case 1

Serial #	Frame Name	Frame Quality No.	Entropy(1)
1	D1	10	2.789122328
2	D4	9	2.654814448
3	D13	8	2.530076643
4	V1	7	2.251143743
5	V3	6	2.148155278
6	H1	5	2.0697226
7	V9	4	2.052080426
8	H2	3	1.977291097
9	H5	2	1.890878138
10	A1	1	1.268929942

Table 2: Energy in decreasing order along with respective frame for patient 1 case 1

Serial #	Frame Name	Frame Quality No.	Energy(E)
1	A1	10	1.23E+08
2	H5	9	5.66E+05
3	H2	8	5.66E+05
4	H1	7	5.66E+05
5	V9	6	4.05E+05
6	V3	5	4.05E+05
7	V1	4	4.05E+05
8	D13	3	6.68E+04
9	D4	2	6.68E+04
10	D1	1	6.68E+04

Patient 1, Case 2 readings

Table 3. Entropy in decreasing order along with respective frame for patient 1 case 2

Serial #	Frame Name	Frame Quality No.	Entropy(I)
1	D1	10	2.7532219
2	D4	9	2.620669182
3	D13	8	2.497562747
4	V1	7	2.239847845
5	V3	6	2.137475261
6	V9	5	2.041967185
7	H1	4	1.99504392
8	H2	3	1.906514512
9	H5	2	1.82370609
10	A1	1	1.289991076

Table 4. Energy in decreasing order along with respective frame for patient 1 case 2

Serial #	Frame Name	Frame Quality No.	Energy(E)
1	A1	10	1.38E+08
2	H5	9	7.19E+05
3	H2	8	7.19E+05
4	H1	7	7.19E+05
5	V9	6	3.28E+05
6	V3	5	3.28E+05
7	V1	4	3.28E+05
8	D13	3	6.36E+04
9	D4	2	6.36E+04
10	D1	1	6.36E+04

I have two cases of patient 1 so now i proceed towards the next patient. It may be noted here that the ordering of frames in entropy and energy tables 3 and 4 respectively is inverse of each other. For the patient 2 there are also two cases, so the readings and

arrangement of the entropy and energy of first 10 WPFs are given in the following Tables.

Patient 2, Case 1 readings

Table 5: Entropy in descending order along with respective frame for patient 2 case 1

Serial #	Frame Name	Frame Quality No.	Entropy(I)
1	D1	10	1.959929854
2	D4	9	1.863807007
3	D13	8	1.774733065
4	H1	7	1.668653671
5	V1	6	1.600354595
6	H2	5	1.589431404
7	V3	4	1.52473708
8	H5	3	1.515828959
9	V9	2	1.454458695
10	A1	1	1.165117955

Table 6: Energy in descending order along with respective frame for patient 2 case 1

Serial #	Frame Name	Frame Quality No.	Energy(E)
1	A1	10	7.32E+07
2	H5	9	9.03E+05
3	H2	8	9.03E+05
4	H1	7	9.03E+05
5	V9	6	8.27E+05
6	V3	5	8.27E+05
7	V1	4	8.27E+05
8	D13	3	1.18E+05
9	D4	2	1.18E+05
10	D1	1	1.18E+05

However in this case the ordering of subbands as per there energy and entropy values is not inverse as H1 is ranked higher in terms of both energy and entropy values as seen in Tables 5 and 6.

Patient 2, Case 2 readings

Table 7 Entropy indices in order alongwith respective frame for patient 2 case 2

Serial #	Frame Name	Frame Quality No.	Entropy(I)
1	D1	10	1.866253621
2	D4	9	1.77430963
3	D13	8	1.689145374
4	H1	7	1.589486285
5	V1	6	1.550707716
6	H2	5	1.513411022
7	V3	4	1.477033911
8	H5	3	1.44278631
9	V9	2	1.40859753
10	A1	1	1.092834182

Table 8 Energy indices in order alongwith respective frame for patient 2 case 2

Serial #	Frame Name	Frame Quality No.	Energy(E)
1	A1	10	7.33E+07
2	V9	9	7.64E+05
3	V3	8	7.64E+05
4	V1	7	7.64E+05
5	H5	6	6.69E+05
6	H2	5	6.69E+05
7	H1	4	6.69E+05
8	D13	3	8.61E+04
9	D4	2	8.61E+04
10	D1	1	8.61E+04

I have two cases of each patient so now i proceed towards the patient 3. For the patient 3 there are also two cases, so the readings and arrangement of the entropy and energy of first 10 WPFs are given in the following Tables 9 and 10.

Patient 3, Case 1 readings

Serial #	Frame Name	Frame Quality No.	Entropy(I)
1	D1	10	1.70877631
2	D4	9	1.623198115
3	D13	8	1.544042971
4	H1	7	1.527035432
5	H2	6	1.452146724
6	V1	5	1.419365868
7	H5	4	1.382767891
8	V3	3	1.350603871
9	V9	2	1.286841491
10	A1	1	1.082192034

Serial #	Frame Name	Frame Quality No.	Energy(E)
1	A1	10	1.27E+08
2	V9	9	1.47E+05
3	V3	8	1.47E+05
4	V1	7	1.47E+05
5	H5	6	8.31E+04
6	H2	5	8.31E+04
7	H1	4	8.31E+04
8	D13	3	9.26E+03
9	D4	2	9.26E+03
10	D1	1	9.26E+03

Patient 3, Case 2 readings

Table 11: Entropy in descending order along with respective frame for patient 3 case 2

Serial #	Frame Name	Frame Quality No.	Entropy(l)
1	D1	10	1.87285193
2	D4	9	1.781118508
3	D13	8	1.696107401
4	V1	7	1.525174598
5	H1	6	1.496717779
6	V3	5	1.453273723
7	H2	4	1.426618113
8	V9	3	1.386440941
9	H5	2	1.36142421
10	A1	1	1.10132868

Table 12: Energy in descending order along with respective frame for patient 3 case 2

Serial #	Frame Name	Frame Quality No.	Energy(E)
1	A1	10	1.18E+08
2	V9	9	7.58E+05
3	V3	8	7.58E+05
4	V1	7	7.58E+05
5	H5	6	5.13E+05
6	H2	5	5.13E+05
7	H1	4	5.13E+05
8	D13	3	1.06E+05
9	D4	2	1.06E+05
10	D1	1	1.06E+05

Now for final selection of useful WPFs i collect the selected frames of each patient and arrange them in the form of a table. In this way i can easily view the common WPFs for each case and select them for further processing.

3.5.5. All selected WPFs for entropy value

The detail of each case of patients is explained in the above tables. So the selected WPFs are given in Table 13, arranged based upon their frame quality. In the following table frame quality is written as '#'.

Table 13. Entropy based selected WPFs along with their frame quality numbers

Patient 1				Patient 2				Patient 3			
Case 1		Case 2		Case 1		Case 2		Case 1		Case 2	
Name	#	Name	#	Name	#	Name	#	Name	#	Name	#
D1	10	D1	10	D1	10	D1	10	D1	10	D1	10
D4	9	D4	9	D4	9	D4	9	D4	9	D4	9
D13	8	D13	8	D13	8	D13	8	D13	8	D13	8
V1	7	V1	7	H1	7	H1	7	H1	7	V1	7
V3	6	V3	6	V1	6	V1	6	V1	6	H1	6
H1	5	V9	5	H2	5	H2	5	H2	5	V3	5
V9	4	H1	4	V3	4	V3	4	V3	4	H2	4
H2	3	H2	3	H5	3	H5	3	H5	3	V9	3
H5	2	H5	2	V9	2	V9	2	V9	2	H5	2
A1	1	A1	1	A1	1	A1	1	A1	1	A1	1

3.5.6. All selected WPFs from energy value

The detail of each case of patients is explained in the above tables. So the selected WPFs are given in Table 14 arranged based upon their frame quality. In the following table frame quality is written as '#'.

Patient 1				Patient 2				Patient 3			
Case 1		Case 2		Case 1		Case 2		Case 1		Case 2	
Name	#	Name	#	Name	#	Name	#	Name	#	Name	#
A1	10	A1	10	A1	10	A1	10	A1	10	A1	10
H5	9	H5	9	H5	9	V9	9	V9	9	V9	9
H2	8	H2	8	H2	8	V3	8	V3	8	V3	8
H1	7	H1	7	H1	7	V1	7	V1	7	V1	7
V9	6	V9	6	V9	6	H5	6	H5	6	H5	6
V3	5	V3	5	V3	5	H2	5	H2	5	H2	5
V1	4	V1	4	V1	4	H1	4	H1	4	H1	4
D13	3	D13	3	D13	3	D13	3	D13	3	D13	3
D4	2	D4	2	D4	2	D4	2	D4	2	D4	2
D1	1	D1	1	D1	1	D1	1	D1	1	D1	1

From these two tables (Table 13, Table 14) i add the frame quality of each respective frame and make this final conclusion of useful WPFs as given in Table 15.

3.5.7. Selected WPFs are used for further analysis

Entropy based selected WPFs		Energy based selected WPFs	
Frame Name	Frame Quality	Frame Name	Frame Quality
D1	60	A1	60
D4	54	H5	45
[redacted]	48	H2	39
V1	39	[redacted]	33
[redacted]	29	[redacted]	45
[redacted]	36	[redacted]	39
[redacted]	18	V1	33
H2	25	[redacted]	18
H5	15	D4	12
A1	6	D1	6

Now i add the frame quality number of respective frame and arrange them in decreasing frame quality numbers.

Frame Name	Total Frame Quality
V1	72
H1	69
V3	68
A1	66
D1	66
D4	66
D13	66
H2	64
V9	63
H5	60

I select the useful WPFs on the basis of higher sums of entropy and energy frame quality. So the upper 8 selected useful WPFs are V1, H1, V3, A1, D1, D4, D13 and H2 as they have higher numbers in terms of frame quality. H5 and V9 are not considered in further analysis because as discussed earlier and depicted in Figure 8 they represent information which is very similar. It may be noted here that the frames which are consistently ranked higher for different MRI images are selected for further analysis.

3.6. Normalization

At this stage the range of intensity values of these WPFs is very large. To maintain the specific range of intensity values normalization of each selected frame is performed. This step is also an important step for making WPFs suitable for further processing particularly because K-means is sensitive to variation in features value range. I use the normalization technique called min-max normalization.

3.7. Min Max Normalization

The next step was to normalize each frame in the range of 0 to 255 for better clustering as K-means is sensitive to the range of values. For this i have used min-max normalization. Min-max normalization transforms a value 'A' to 'B' which fits in the range [C, D]. It is given by the Equation 11.

$$B = \left(\frac{(A - \min imum\ value\ of\ A)}{(\max imum\ value\ of\ A - \min imum\ value\ of A)}\right) * (D - C) + C \qquad (11)$$

In the Equation 11, 'A' represent the present pixel intensity value and 'C' indicate the new lower limit of intensity value and 'D' the upper limit of the intensity value.

3.8 Clustering

Clustering is a machine learning method which is used to place data elements into related groups or classes. One of the oldest and widely used clustering techniques includes K-means clustering [2]. The elements of data set are clustered based upon shared properties.

The study of over all data becomes very easy after clustering. The selection of clustering technique is dependent on type and especially the size data set. To understand the concept of clustering some graphical representations are given in Figure 9.

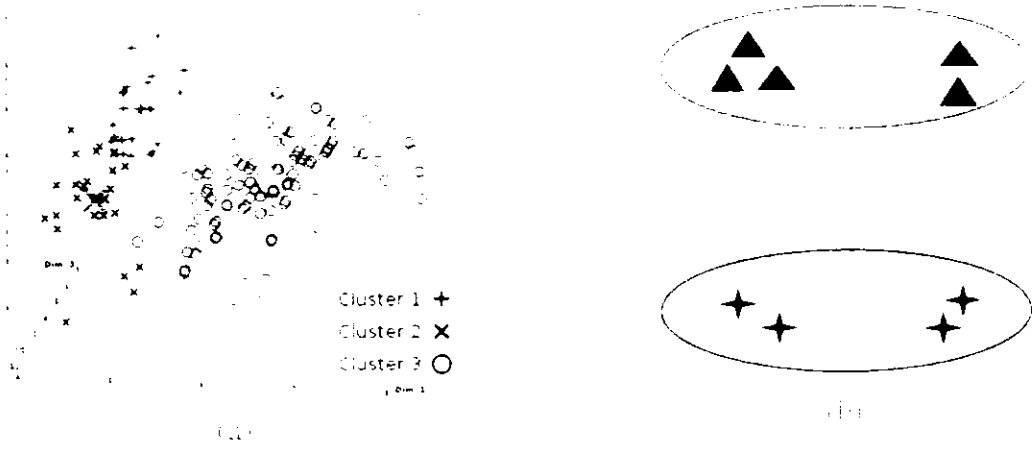

Figure 9: (a) Clustering of three different shapes in 3D frame and figure (b) shows the two different shapes in 2D plane.

Figure 9 shows the example of clustering on the basis of objects shape. In this figure same looking objects are clustered together with same color.

3.8.1. Importance of Clustering

Clustering has been used in different fields of science for a long time. The importance of clustering can be judged by taking a look at its use in the last few years. Search at Google scholar [48] shows, more than 1660 entries for data clustering in year 2007. In the field of engineering and medical sciences, data clustering is used for image segmentation [1, 3]. Different clusters are generated on the basis of density value, energy value, shape and size [3]. In computer vision and image processing, the most important characteristic is

intensity of pixels for differentiating between clusters. The main target of clustering is to decrease the amount of data by grouping similar data together. K-means clustering is also very useful for data mining [49].

3.8.2. Some possible applications of data clustering algorithm

Marketing: Finding groups of customers with similar behavior given a large database of customer data containing their properties and past buying records.

Biology: Classification of plants and animals given their features.

Medical image data base: for detail see [3, 49].

3.9. K-means clustering

3.9.1 Definition

K-means clustering is an algorithm that attempts to locate groups in data [50].

K-means clustering is a simple method for unsupervised categorization. The K-means algorithm is commonly used in medical imaging and biometrics. In K-means clustering K denotes the number of clusters. In K-means clustering, i need to define in advance the number of clusters i intend to acquire from a data-set.

3.9.2. The K-means Algorithm

The K-means clustering arranges the data into K groups. The value of K is provided as an input parameter. It examines every component of data set and assigns it to one of the clusters depending on the minimum distance from the cluster center. The position of

centroids is recalculated every time a component is added to the cluster. This step continues until all the components are grouped in to a final number of required clusters. In every iteration, the algorithm attempts to decrease the mean distance between data points and centroids. The mathematical form is as Equation 12.

$$V = \sum_{i=1}^{k} \sum_{x_j \in S_i} (x_j - \mu_i)^2 \tag{12}$$

In the above Equation 12, the "K" represents the number of clusters where "i" is an integer from 1 to k. The "μ" represents the mean. The K mean clustering algorithm follows these steps

1) First place K points to the space represented by objects which are being clustered.
2) Allot each object to group that has nearest centroid.
3) Recalculate the mean distance of the K centroids.
4) Repeat steps 2 & 3 until the resultant centroids no longer change.
5) Cluster the points which are based on mean distance.

$$c^{(i)} = \arg\min_j \left\| x^{(i)} - \mu_j \right\|^2 \tag{13}$$

6) Comparing of new centroids with each cluster.

$$\mu_i = \frac{\sum_{i=1}^{m} 1\{c_{(i)} = j\} x_i}{\sum_{i=1}^{m} 1\{c_{(i)} = j\}} \tag{14}$$

In the above equation "j" iterates over all centroids and the "i" iterates over all mean distances. The three input parameters to K-means clustering algorithm in MATLAB are:

- Value of "K": The value of 'K' shows the number of cluster. If the value of K=3, then total three clusters are formed.

- Replicates: Number of times to repeat the clustering, each with a new set of initial cluster centroid positions. I am using the value of replication= 5.

- Distance function: I am dealing with two types of distances named as squared Euclidean distance and city block. In the K-means clustering the squared Euclidean distance is used as default distance. As a result of using this distance, K-means can finds spherical clusters in the data [5]. I use these two distances and compare their results with K-means clustering results on raw images and on selected WPFs.

3.9.3. City block distance function

The city block distance is also known as Manhattan distance or absolute value distance. The measurement of cityblock distance would be zero only for two identical points. It gives higher value when there is some dissimilarity between points [51]. The mathematical formula to calculate cityblock distance is shown in Equation 15.

$$d = \sum_{i=1}^{k} \left| x_i - y_i \right| \tag{15}$$

The above Equation 15 shows the formula to calculate cityblock distance.

3.9.4. Euclidean distance function

The squared Euclidean distance is the sum of the squared difference between readings for two cases on all variables. Mathematically it referred as Equation 16.

$$d = \sum_{i=1}^{k} \left(x_i - y_i \right)^2 \tag{16}$$

3.10. Conclusion and Summary

In this chapter first I describe the data set used for analysis. Then i provided the details pertaining the formation of DWPF and described my technique. Computing energy and entropy for each Wavelet Packet Frame (WPF) and selecting useful WPFs according to proposed technique. Then i provide the introduction of K-means clustering which i am using with squared Euclidean distance function and city block distance function. K-mean clustering is next step for disease segmentation. The results of proposed technique are discussed in the next chapter.

CHAPTER# 4

RESULTS AND DISCUSSION

I compare my result with the simple K-means clustering results for evaluation of what improvements can be attained in K-means clustering using my method. In this way, i will prove that my results are better than ordinary K-means clustering. The results would show that using my technique doctors can obtain better visualization of MRI data without using expensive contrast reagents (CRs) as used in the more expensive (Magnetic Resonance Imaging) MRI modality i.e. contrast enhanced MRI. The MRI contrast is used to enhance the visibility of structures (internal body) in MRI. Commonly used compounds for contrast enhancement are Gadolinium (lll) based. This Gadolinium (lll) contrast agents are frequently used for brain tumor MRI contrast enhancement [9].

4.1. Segmented results

The names of some Food and Drug Administration (FDA) approved contrast agents are:

- Gadodiamide (Ominiscan)
- Gadobenic (Multihance)

These types of medicines have their after side effects. With the use of these contrast agents patients may suffer from different conditions such as allergy etc. Some other unknown diseases may occur months after the contrast have been injected [52]. These contrast agents are also very costly. The proposed technique helps the doctors to get good

visualization results without using these costly contrast agents. In this way i can reduce the cost of MRI for patients as well. Some advanced as well as expensive MRI machines are also available which facilitate the doctors to change the contrast of normal MRI images. The proposed technique also facilitates doctors to save that extra cost of buying advanced MRI machines. In the results, the original names of patients are not mentioned due to patient privacy issue.

4.2. Patients and their Diseases

There are total three patients whom i would refer to as patient 1, patient 2 and patient 3. I start from patient1. Every patient has two cases. The data set is collected from PIMS hospital Islamabad. I also collect medical reports of each patient along with data set. After the completion of my results, i discussed my results with the collaborating physician from PIMS hospital. He was impressed by my results and asked us to incorporate it in to medical imaging data viewing stations at PIMS. The abnormalities in the MRI images of these patients according to the doctor's report are given in Table 17.

Table 17: Patients and their diseases

Serial #	Patient Number	Disease
1	Patient 1	This patient suffering from tumor or non-enhancing mass in right side of the brain.
2	Patient 2	Grid of membrane appears in left side of brain due to infection.
3	Patient 3	The appearances of mass lesion in left parietal region.

4.3. Patients and their results

Figure 10 shows original image of patient 1, case 1

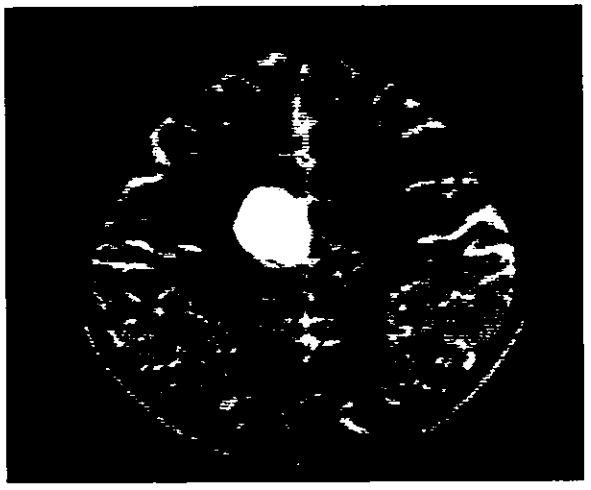

(a)

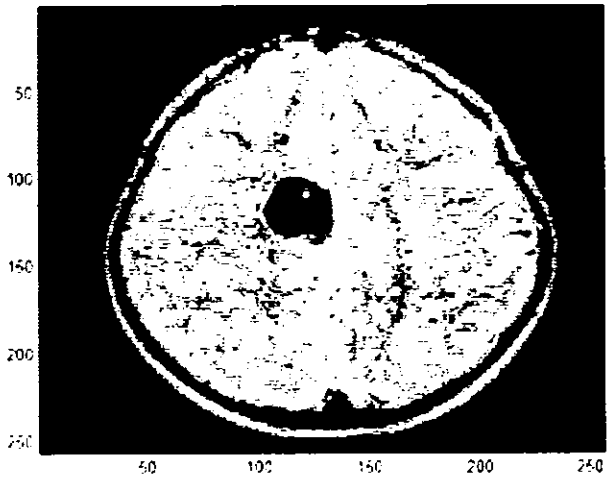

(b)

Figure 10: (a) Original grey scale image of patient 1, case 1 (b) [illegible] image with color map [illegible]

Now the results of this patient for K=2, K=3 and K=4 are shows in Figure 11, Figure 12 and Figure 13 respectively.

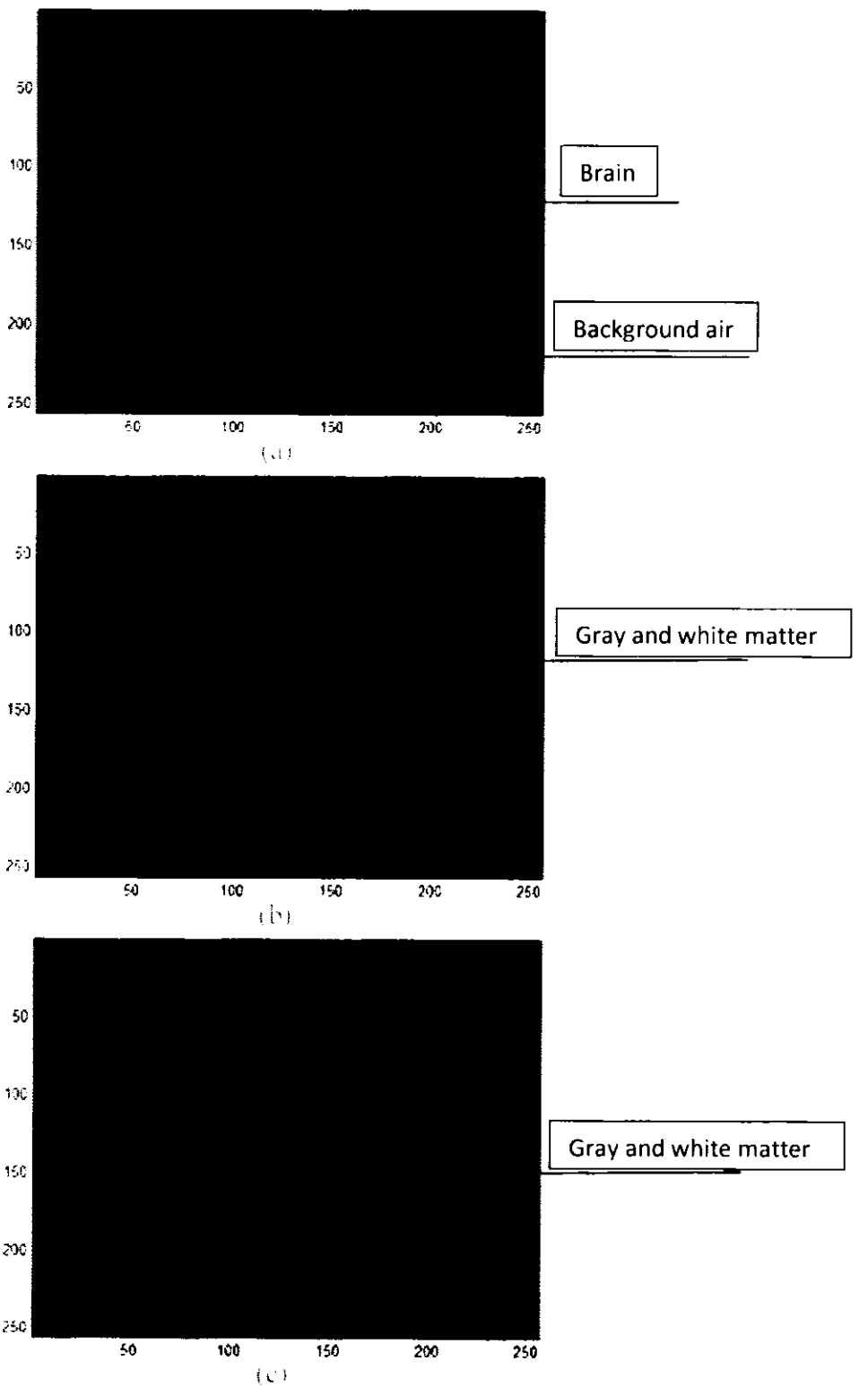

...ent 1, case 1. (a) Simple K-means clustering at K = 2, (b) K-means ...ared Euclidean distance after applying DWPF and (c) K-means ... block distance after applying DWPF.

Figure 11 shows the results after K-means clustering. In this Figure 11 i set the numbers of clusters as 2. Figure 11 (a) shows the result of simple K-means clustering, on original MRI image. This does not give any information about the disease of the brain. It only segments the brain from the surrounding air. Figure 11 (b) shows the result of my proposed technique using squared Euclidean distance function in K-means clustering. The result is improved because it also gives information about the position of gray and white matter of brain. Figure 11(c) shows the result of my proposed technique using cityblock distance function in K-means clustering. It also provides better results as compared to the simple K-means clustering. At this stage (K=2), the proposed technique is not providing better results. If i increase the number of clusters it will give better performance.

Figure 12 shows the results after K-means clustering. In this Figure 12 i set the value of K=3, so there will be three clusters in the resultant image. Figure 12 (a) shows the result of simple K-means clustering on original MRI image. At this value of K it gives some information about the gray and white matter of the brain. Figure 12 (b) shows the result of my proposed technique using squared Euclidean distance function in K-means clustering. The result is improved now because i have been able to segment the diseased area in the image. The information of gray and white matter also appears. Figure 12 (c) shows the result of my proposed technique using cityblock distance function in K-means clustering. In this result the information of gray and white matter appears individually but not very clear and the diseased segment is also not very apparent.

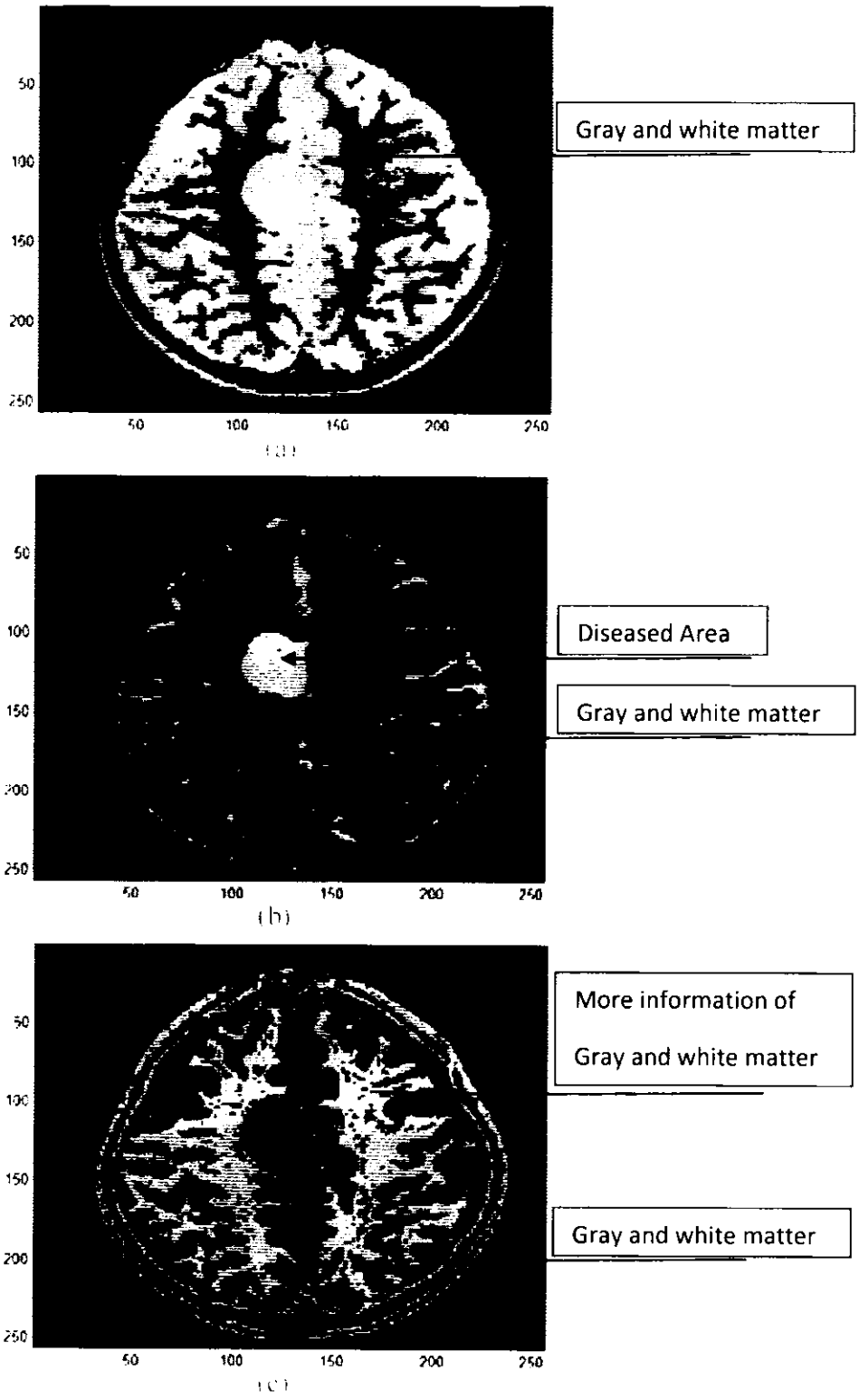

Patient 1 case 1 (a) Simple K-means clustering (K=3) using squared Euclidean distance after applying DWT (b) Clustering using cityblock distance after applying DWT

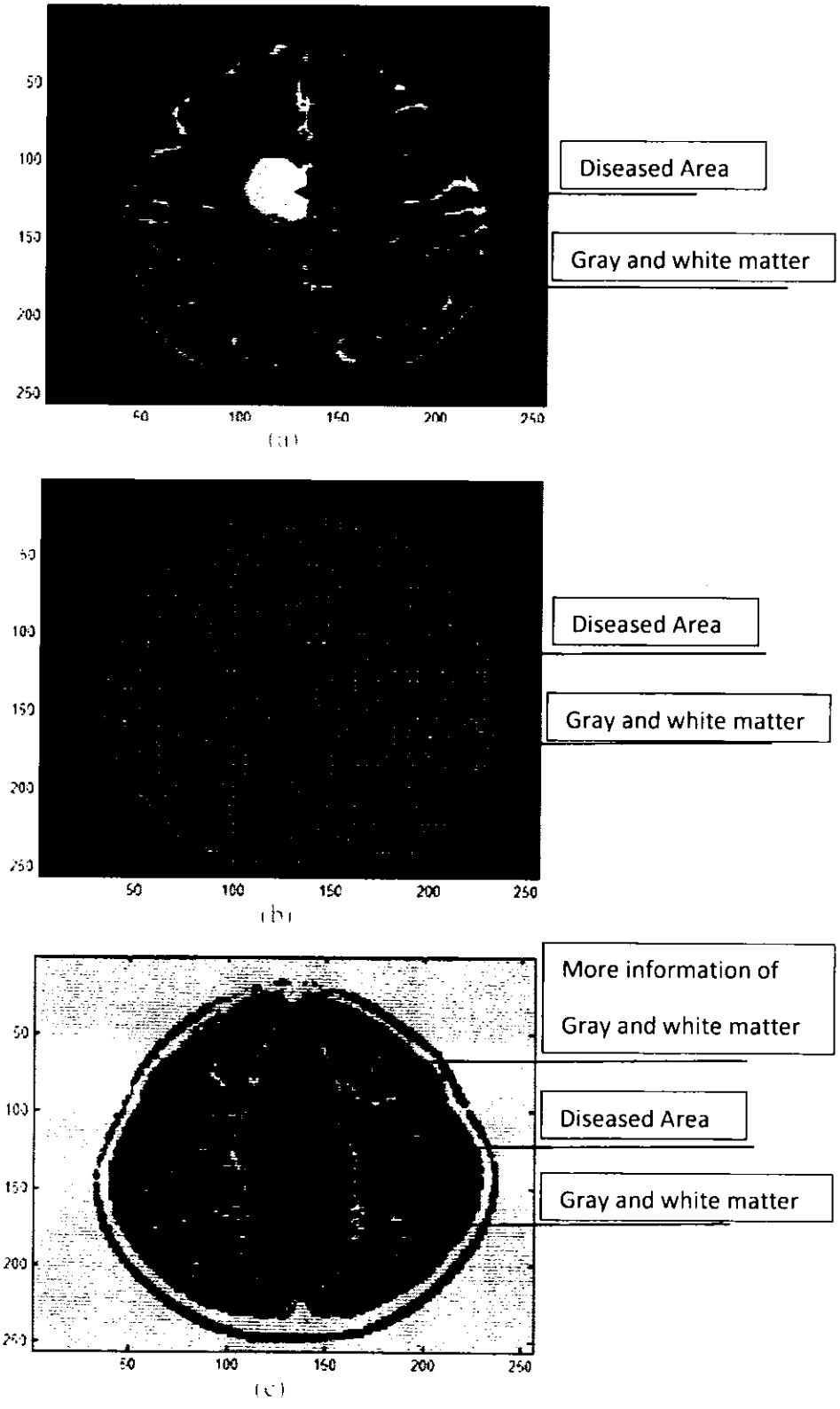

[illegible] case I. (a) Simple K-means clustering at K [illegible] K-means [illegible] squared Euclidean distance after applying DWPT and [illegible] K-means [illegible] block distance after applying DWPT

In this Figure 13 i increase the number of clusters from three to four, so K=4. Figure 13 shows the results after K-means clustering. Figure 13 (a) shows the result of simple K-means clustering on original MRI image. At this value of K it gives good information about the diseased area along with gray and white matter of the brain. Figure 13 (b) shows the result of my proposed technique using squared Euclidean distance function in K-means clustering. In this image the area of the disease almost remains same but distortion appears and looks like noise. The information of gray and white matter also appears but is not very clear. Figure 13 (c) shows the result of my proposed technique using cityblock distance function in K-means clustering. In this result the information of diseased area becomes clear. The additional information of gray and white matter appears individually and clearly. So the cityblock distance function gives good perform for four numbers of clusters. For the verification of this result, i apply the same technique on data of all other patients.

Figure 14 shows Patient 1, case 2

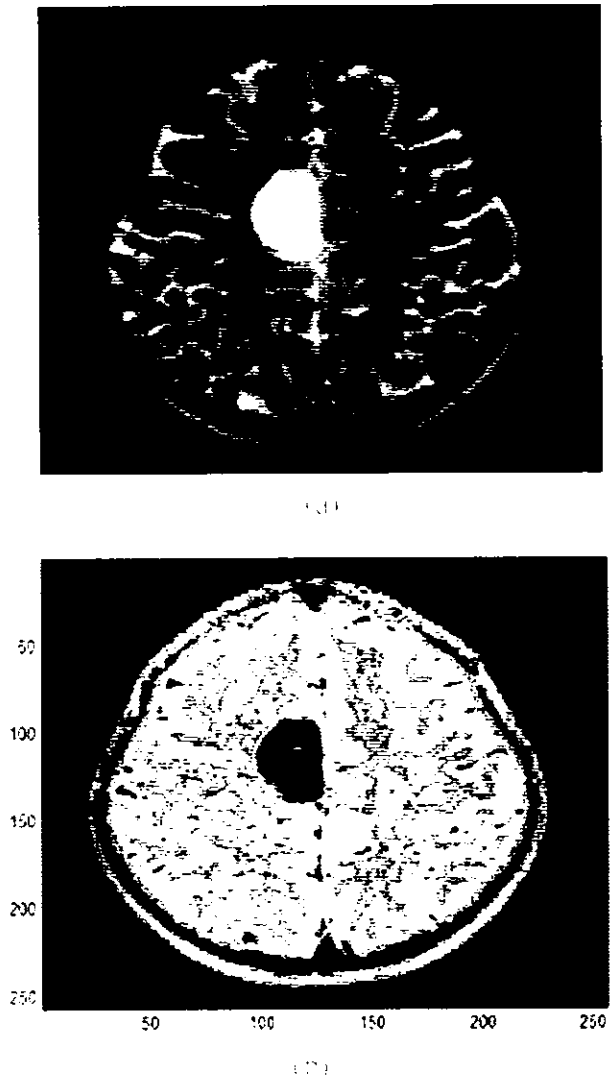

Figure 14: (a) Original gray scale image of patient 1, case 2 and (b) original image with color map jet

Now the results of this patient for K=2, K=3 and K=4 are shows in Figure 15, Figure 16 and Figure 17 respectively.

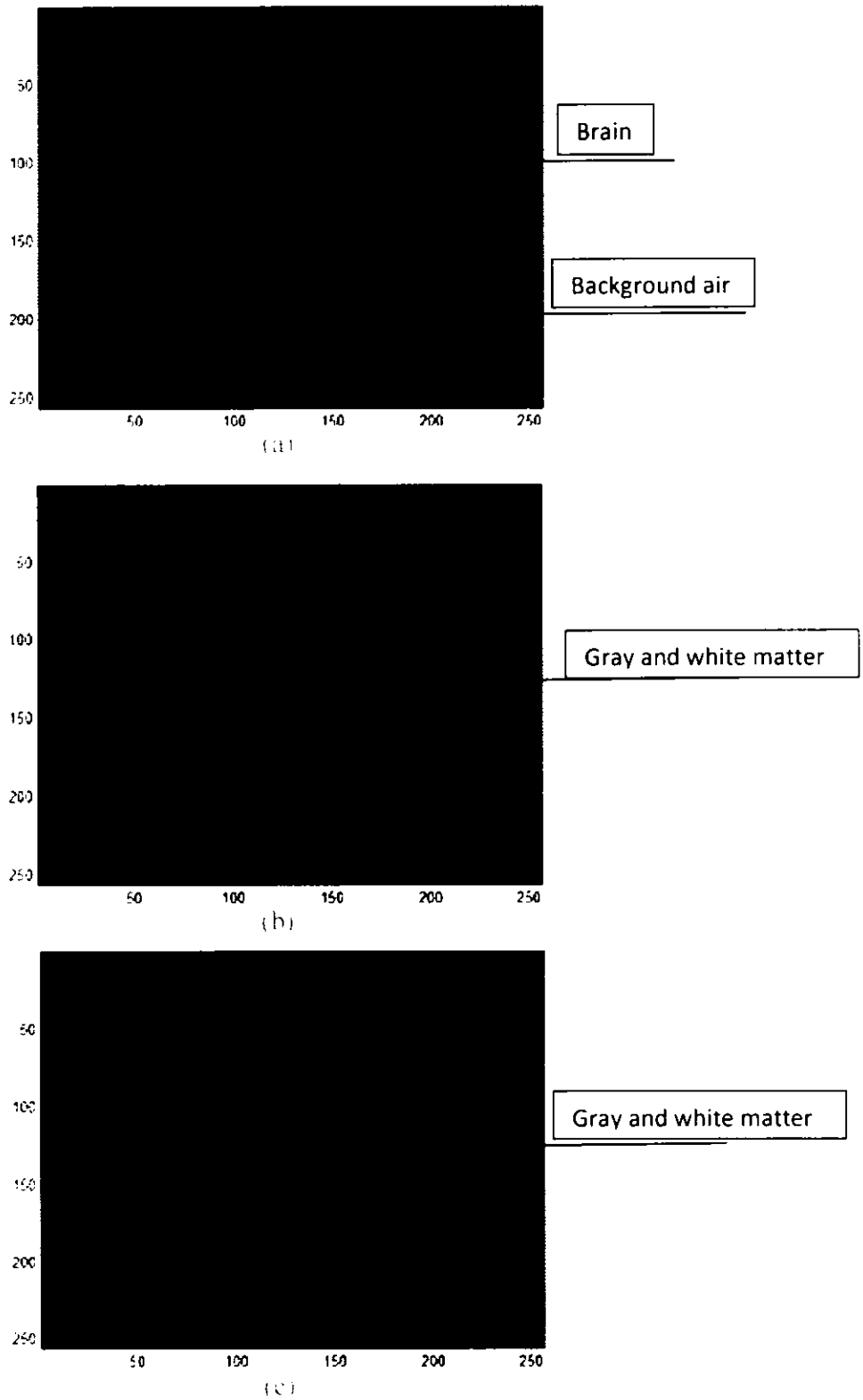

...Simple K-means clustering at K=... squared Euclidean distance after applying DWPT ... K-means ... block distance after applying DWPT.

In Figure 15 i set the numbers of clusters as two. Figure 15 (a) shows the result of simple K-means clustering on original MRI image of patient 1, case 2. This does not give any information about the disease of the brain. It only segments the brain from the surrounding air. The Figure 15 (b) shows the result of my proposed technique using squared Euclidean distance function in K-means clustering at K=2. The result is improved because information about the gray and white matter of brain appears. Figure 15 (c) shows the result of my proposed technique using cityblock distance function in K-means clustering. It also gives some information about gray and white matter but is more valuable as compared to the simple K-means clustering result as segmentation of the gray and white matter region is better. At this stage (K=2), the proposed technique is not providing better results. If i increase the number of K it will give better performance.

The Figure 16 shows the results after K-means clustering. In this Figure 16 i set the value of K=3. The Figure 16 (a) shows the result of simple K-means clustering, on original MRI image. At this value of K it gives some information about the gray and white matter of the brain but lose information about the region of interest (diseased area). The Figure 16 (b) shows the result of my proposed technique using square Euclidean distance function in K-means clustering. The result is improved because now i can also easily mention the diseased area in the image. The information of gray and white matter also appears improved in contrast but not individually. The Figure 16 (c) shows the result of my proposed technique using cityblock distance function in K-means clustering. In this result the information of gray and white matter appears individually. This individual information of gray and white matter is also important for doctors.

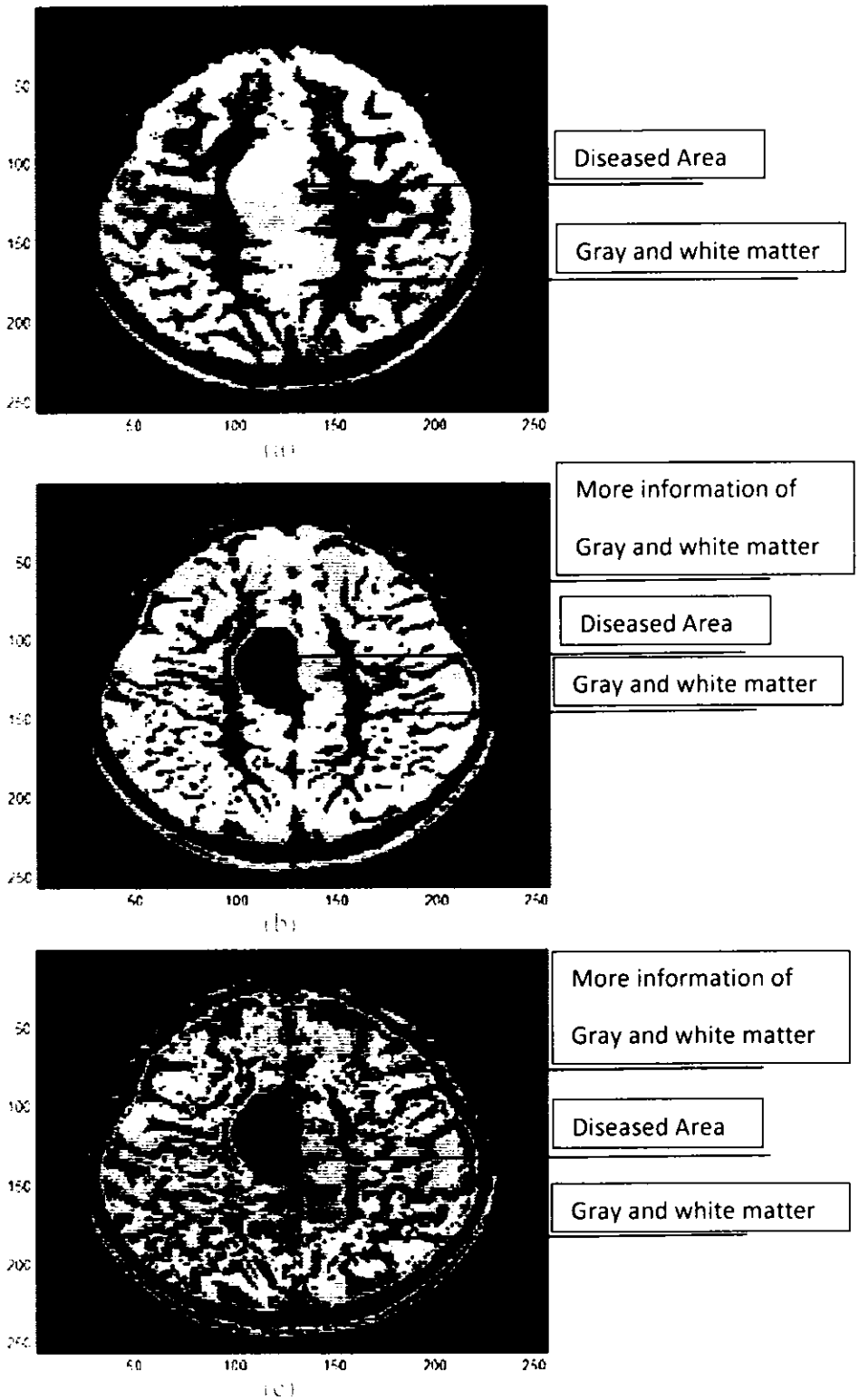

Figure 5.6: Experiment 1, case 2: (a) Simple K-means clustering (b) Fuzzy K-means clustering with squared Euclidean distance after applying DWPT and (c) K-means clustering with city block distance after applying DWPT.

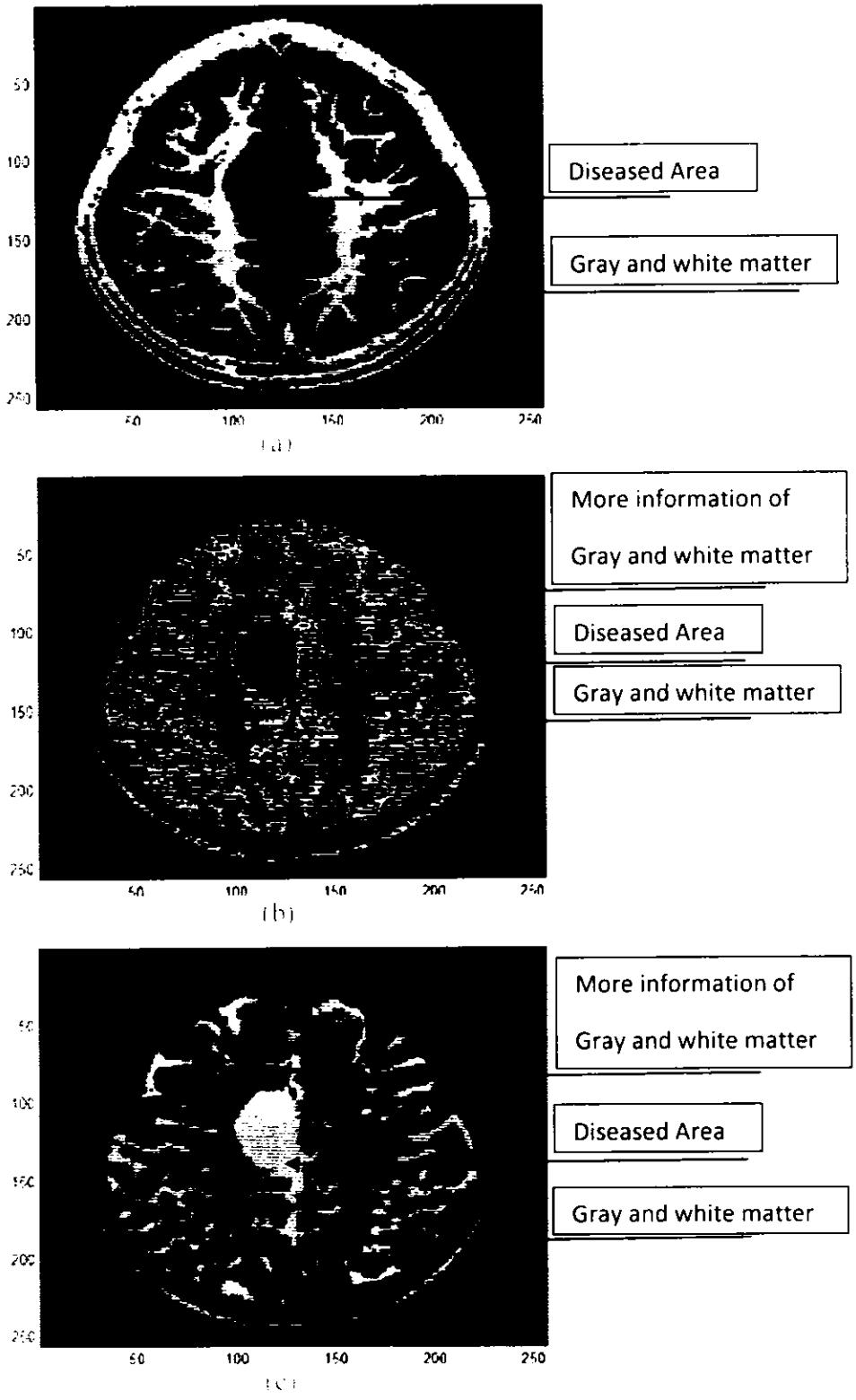

Case 2: (a) Simple K-means clustering at K = [illegible] (b) [illegible] ed Euclidean distance after applying DWPT (c) [illegible] block distance after applying DWPT

In this Figure 17 i increase the number of clusters from three to four, so K=4. Figure 17 shows the results after K-means clustering. Figure 17 (a) shows the result of simple K-means clustering, on original MRI image. At this value of K, it gives good information about the diseased area along with gray and white matter of the brain but the detail of gray and white matter is missing. Figure 17 (b) shows the result of my proposed technique using squared Euclidean distance function in K-means clustering at K=4. In this resultant image the area of the disease almost remains same but the distortion appears on the brain image. The information of gray and white matter also appears but not so clear. Figure 17 (c) shows the result of my proposed technique using cityblock distance function in K-means clustering. In this result the information of diseased area becomes clear. The additional information of gray and white matter appears individually and clearly. So the cityblock distance function gives good perform for four numbers of clusters.

Figure 18 shows Patient 2, case 1

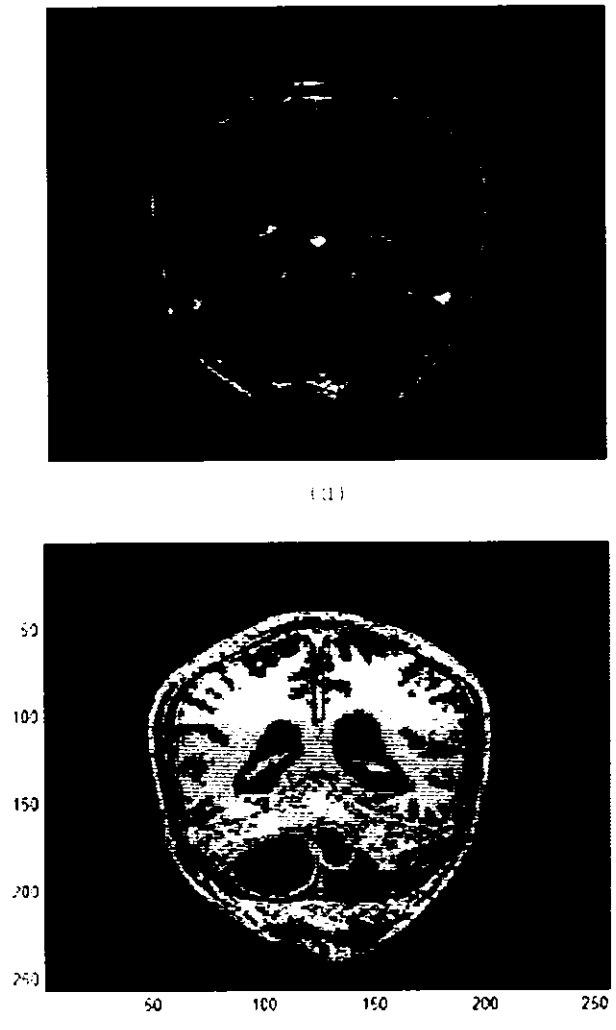

(a)

(b)

Figure 18. (a) Original gray scale image of patient 2, case 1 and (b) segmented image with color map jet

Now the results of this patient for K=2, K=3 and K=4 are shows in Figure 19, Figure 20 and Figure 21 respectively.

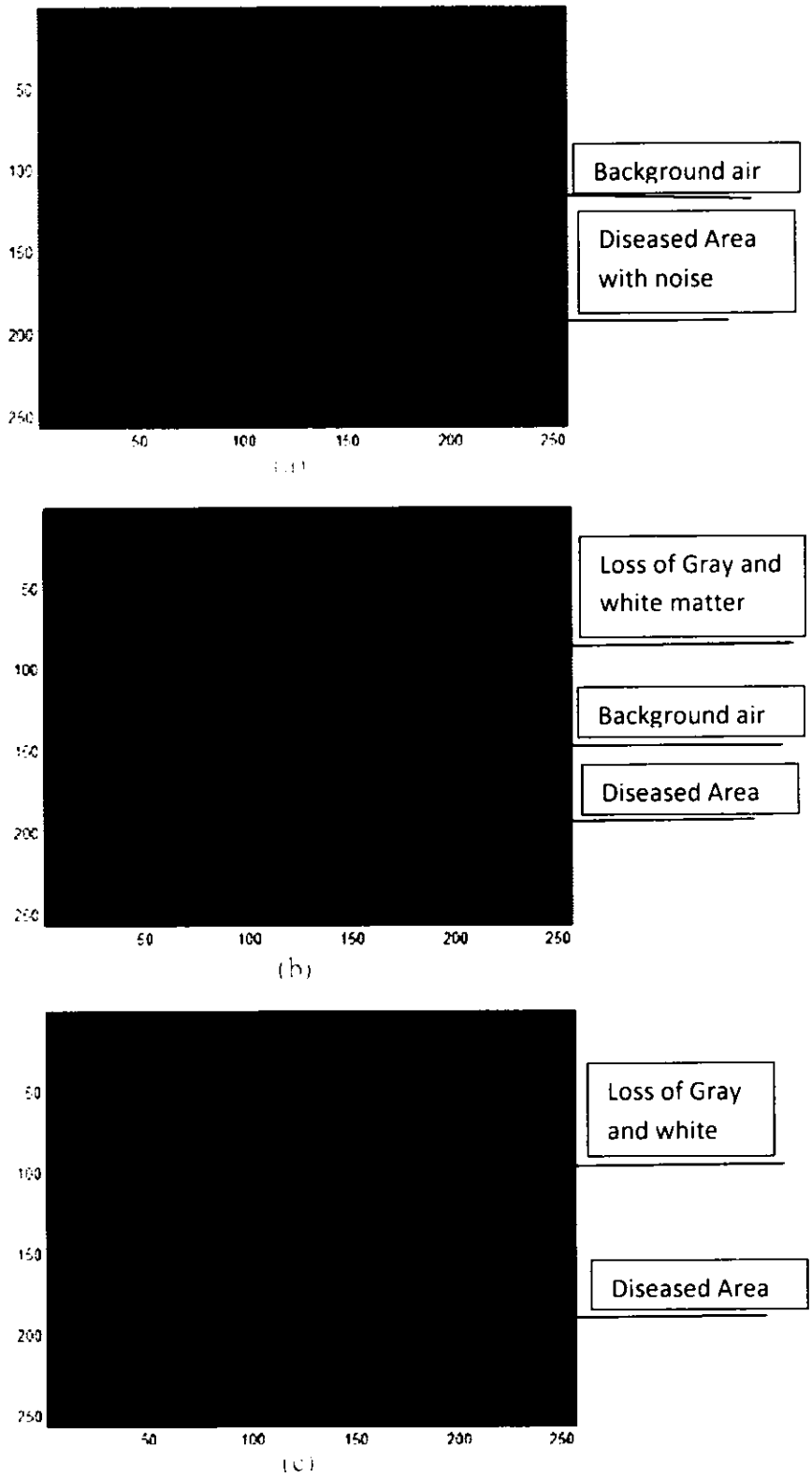

ent 2: ease 1: (a) Simple K-means clustering at K=2, (b) K-means ared Euclidean distance after applying DWPT, (c) K-means ybiock distance after applying DWPT.

Figure 19 shows the results of second patient, case 1 after K-means clustering. In this Figure 19 the total number of clusters are two (K=2). Figure 19 (a) shows the result of simple K-means clustering, on original MRI image. This gives noise in the desired area of interest as mentioned in the Figure 19 (a). Figure 19 (b) shows the result of my proposed technique using squared Euclidean distance function in K-means clustering at K=2. The result is improved because the noise in the diseased area disappears. Figure 19(c) shows the result of my proposed technique using cityblock distance function in K-means clustering. The error in desired area also cleaned up completely. It gives no information about gray and white matter of brain but is more valuable as compare to the simple K-means clustering result at the same number of clusters. For the detail information of gray and white matter of brain i increase the value of K.

Figure 20 shows the results after K-means clustering. In this image i set the numbers of clusters as 3. Figure 20 (a) shows the result of simple K-means clustering, on original MRI image. At this value of K it gives some information about the gray and white matter of the brain but noise appears in the diseased area. Some unaffected tissues also segment as diseased area. Figure 20 (b) shows the result of my proposed technique using squared Euclidean distance function in K-means clustering at K=3. The result is improved now because i have been able to mention the diseased area in the image easily without any noise but the information of gray and white matter still missing. Figure 20 (c) shows the result of my proposed technique using cityblock distance function in K-means clustering. In this result the information of gray and white matter appears individually. This individual information of gray and white matter is also important.

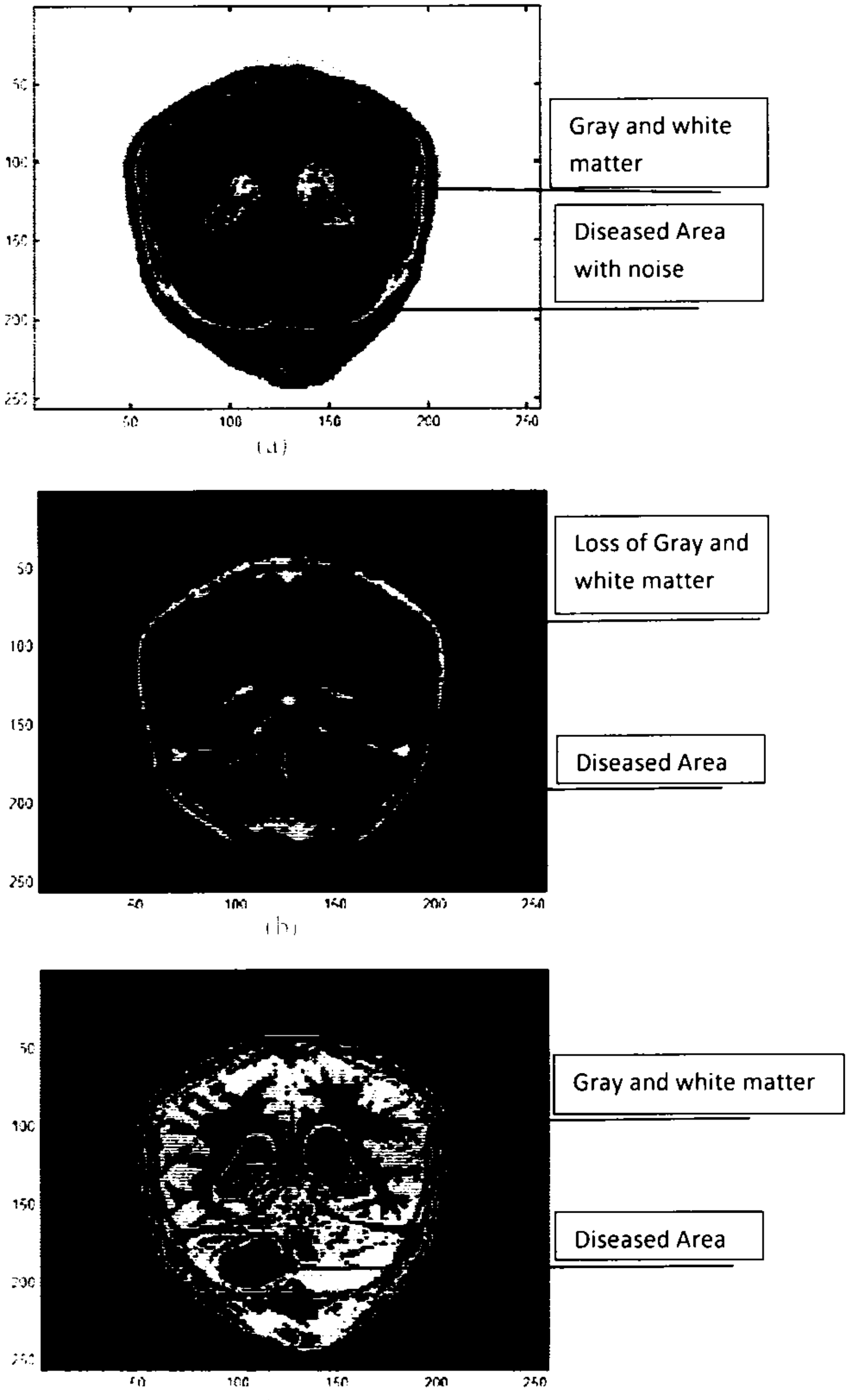

[illegible] ent 2, case 1. (a) Simple K-means clustering at K=3, (b) K-means clustering using squared Euclidean distance after applying DWPF and (c) K-means clustering using cityblock distance after applying DWPF.

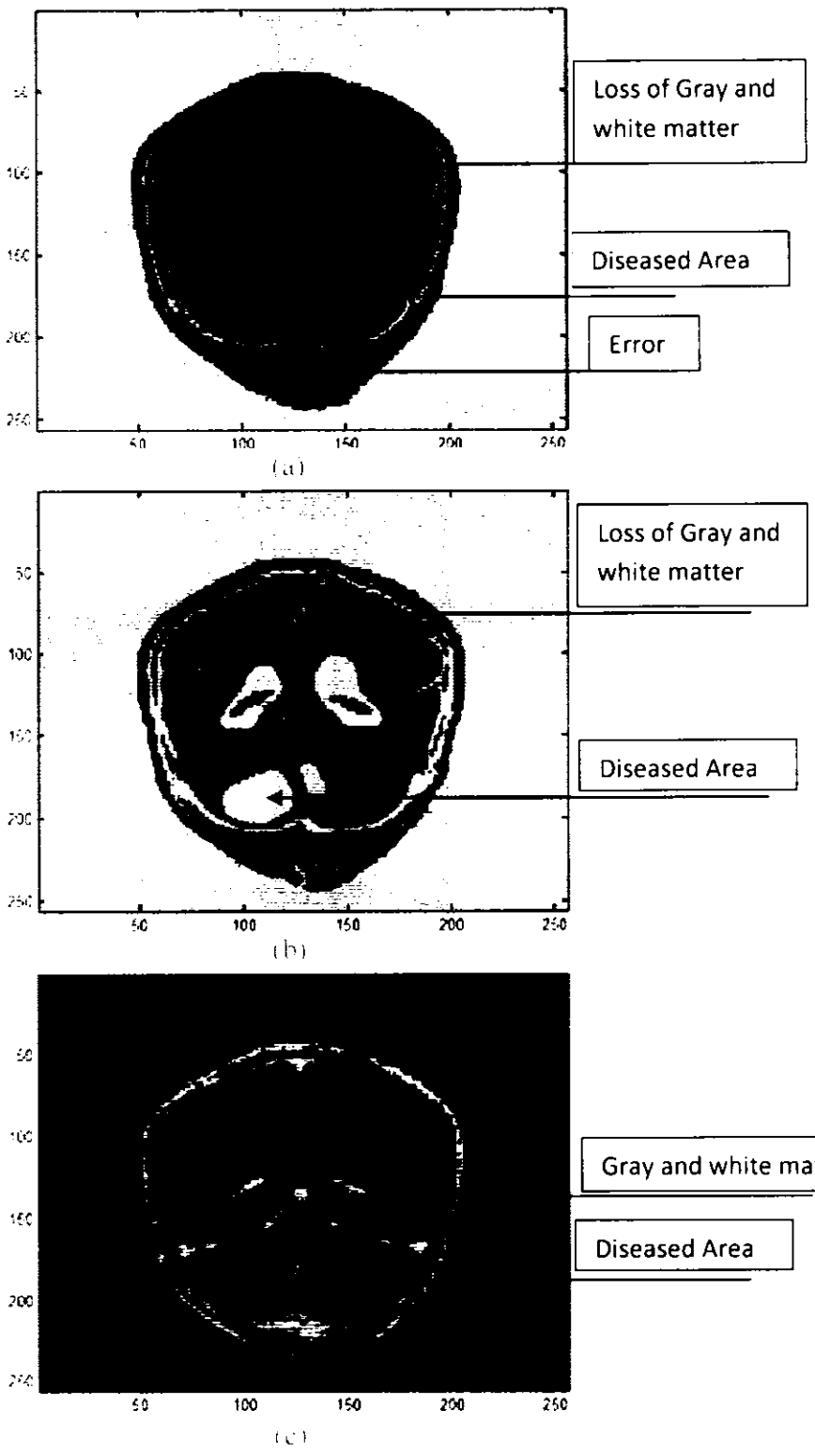

Simple K-means
ared Euclidean distance after applying DWPT and
blood distance after applying DWPT

In this Figure 21 i increase the number of clusters from three to four, so K=4. Figure 21 (a) shows the result of simple K-means clustering, on original MRI image. At this value of K it gives good information about the diseased area. Small errors appear near the diseased area as mentioned in Figure 21 (a). It gives no information about the gray and white matter of the original image. Figure 21 (b) shows the result of my proposed technique using squared Euclidean distance function in K-means clustering at K=4. In this resultant image the area of disease almost remains same but no error appears near diseased area. The information of gray and white matter is missing. Figure 21 (c) shows the result of my proposed technique using cityblock distance function in K-means clustering. In this result the information of diseased area becomes clear from noise. So i have been able to segment the diseased area in the image without computing errors. The additional information of gray and white matter appears individually and clearly. So the cityblock distance function gives good performance when i set numbers of clusters as 4.

Figure 22 shows Patient 2, case 2

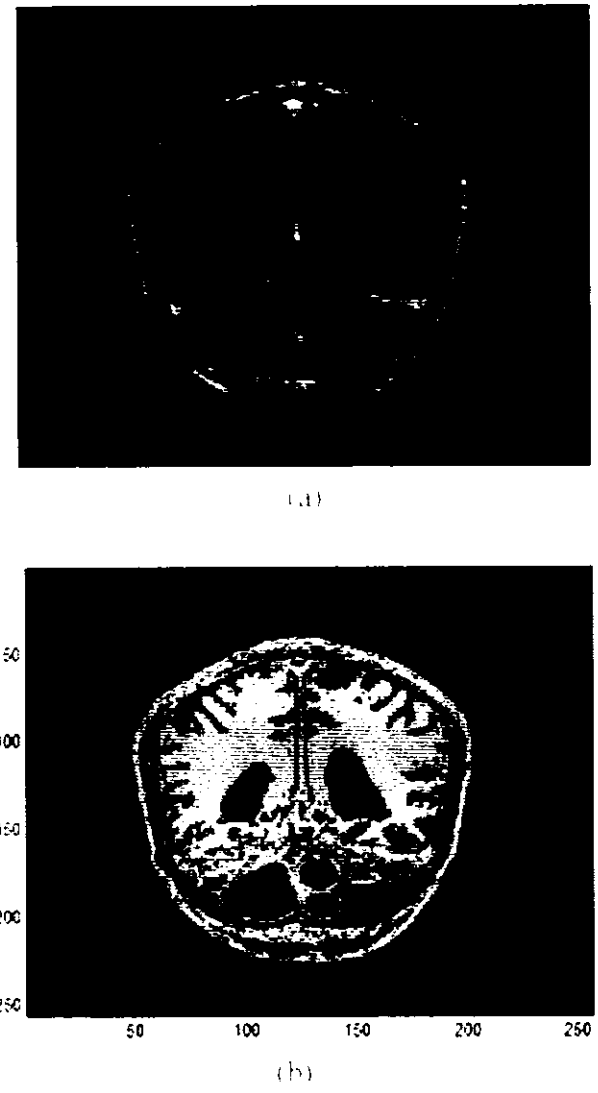

(a)

(b)

Figure 22: (a) Original gray scale image of patient 2, case 2 and (b) original image with color map jet

Now the results of this patient for K=2, K=3 and K=4 are shows in Figure 23, Figure 24 and Figure 25 respectively.

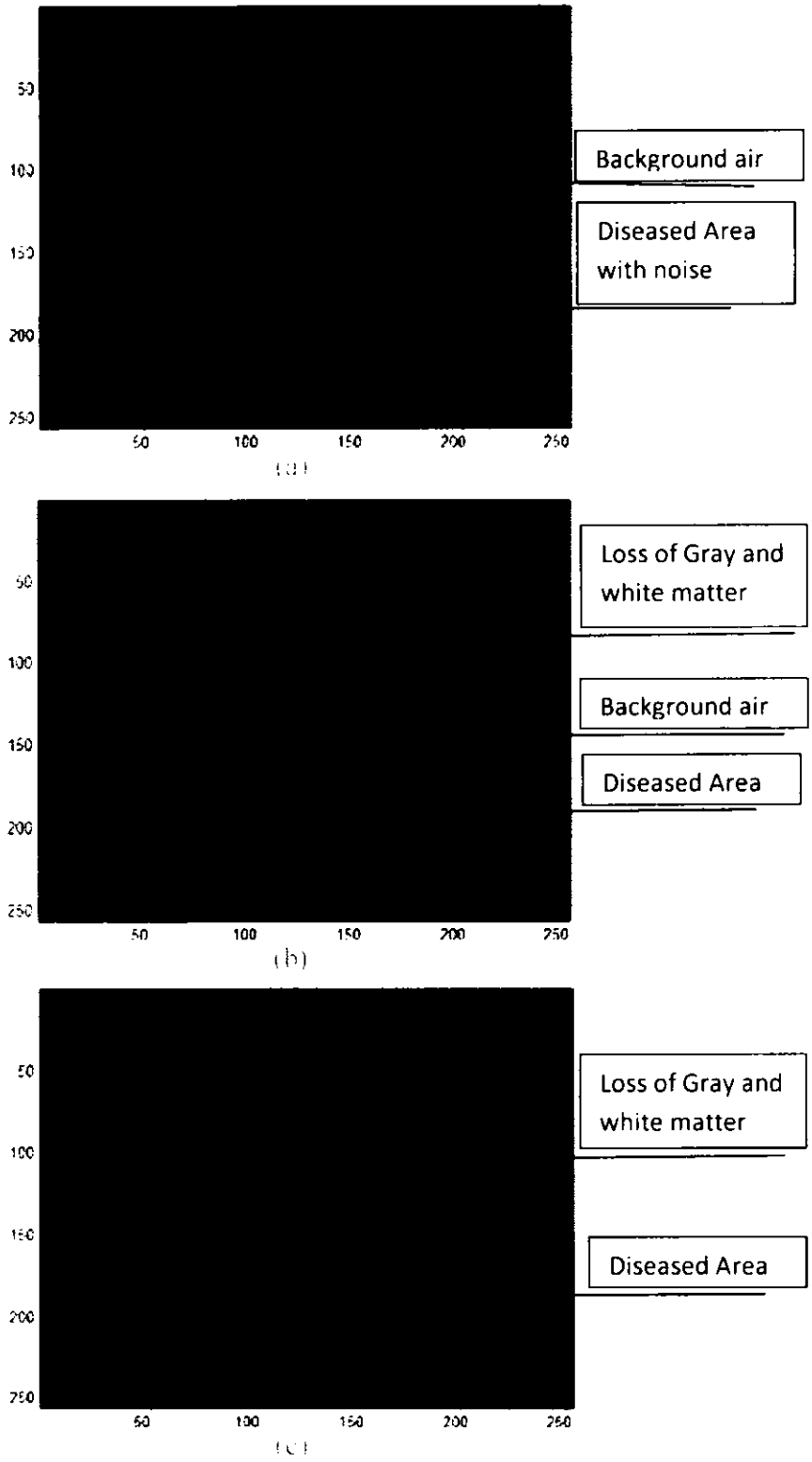

Patient 2 case 2: (a) Simple K-means clustering at K = 2, (b) K-means clustering using squared Euclidean distance after applying DWPT and (c) K-means clustering using cityblock distance after applying DWPT.

In this Figure the total numbers of clusters are two (K=2). Figure 23 shows the results of second patient, case 2 after K-means clustering. Figure 23 (a) gives the result of simple K-means clustering, on original MRI image. This gives noise in the desired area of interest as mentioned in Figure 23 (a). It gives no useful information about the structure of other gray and white matter tissues of brain. Figure 23 (b) shows the result of my proposed technique using squared Euclidean distance function in K-means clustering at K=2. The result is improved now because the noise on the diseased area disappears. Figure 23 (c) shows the result of my proposed technique using cityblock distance function in K-means clustering. The error in desired area also cleaned up completely. Now i have been able to segment the area of interest without noise. It also gives no information about gray and white matter of brain but the result is more valuable as compare to the simple K-means clustering result at the same number of clusters. For the detail information of gray and white matter of brain i increase the value of K.

The Figure 24 shows the results of patient 2, case 2 after K-means clustering. Here i set the numbers of clusters as 3. The result of simple K-means clustering, on original MRI image is shown in the Figure 24 (a). At this value of K it again gives no information about the gray and white matter of the brain but noise appears inside the diseased area as mentioned in Figure 24 (a). Figure 24 (b) shows the result of my proposed technique using squared Euclidean distance function in K-means clustering at K=3. The result is improved now because i have been able to mention the diseased area in the image without any inside noise but the information of gray and white matter is still missing. Figure 24 (c) shows the result of my proposed technique using cityblock distance

function in K-means clustering. In this result the diseased area appears with sharp edges as compare to result of simple K-means clustering. For the information about gray and white matter i need to increase the number of clusters (K) in the resultant image.

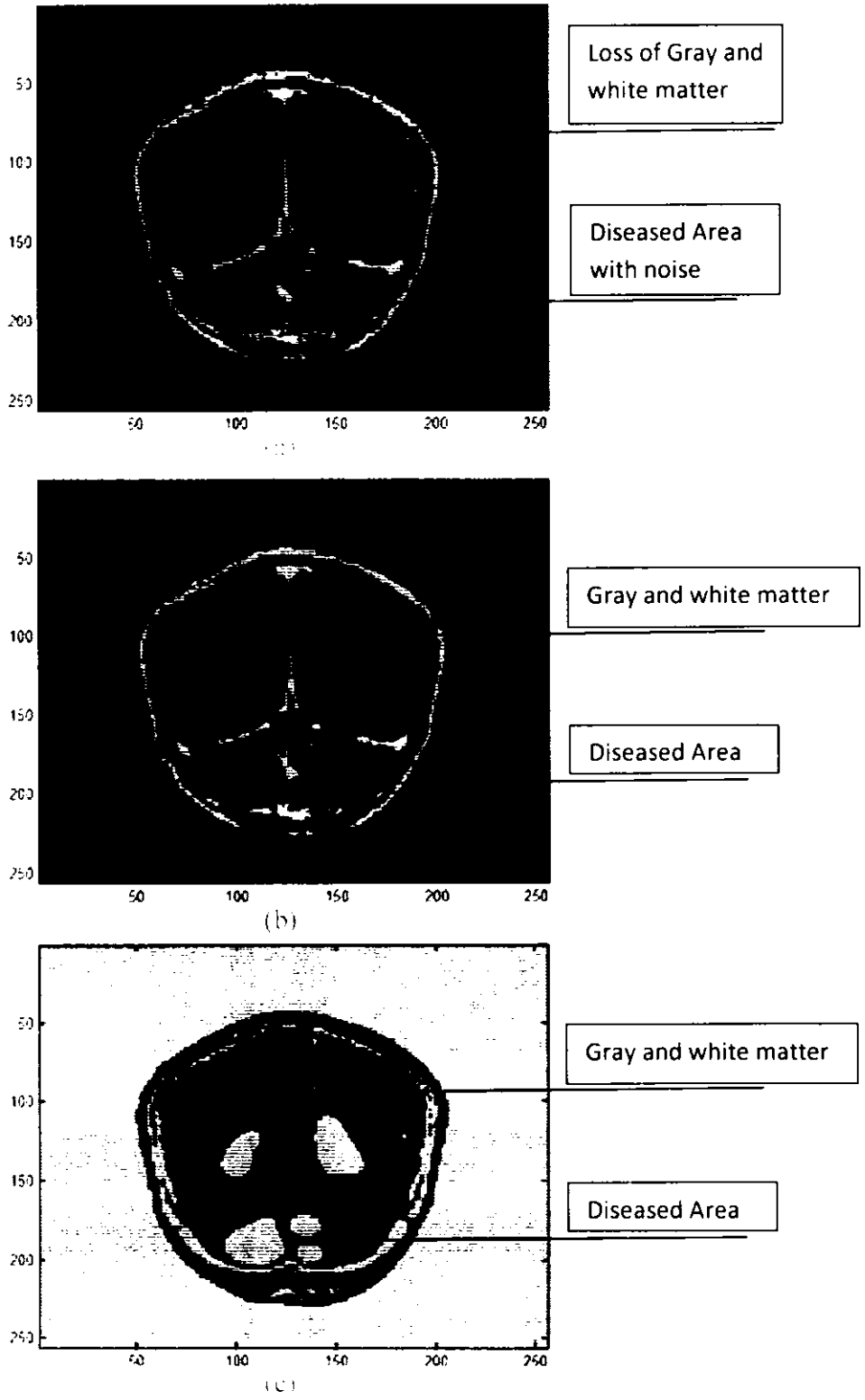

[illegible] ment 2, case 2, (a) Simple K-means clustering at k=3, (b) K-means [illegible] squared Euclidean distance after applying DWPT and (c) K-means [illegible] cityblock distance after applying DWPT.

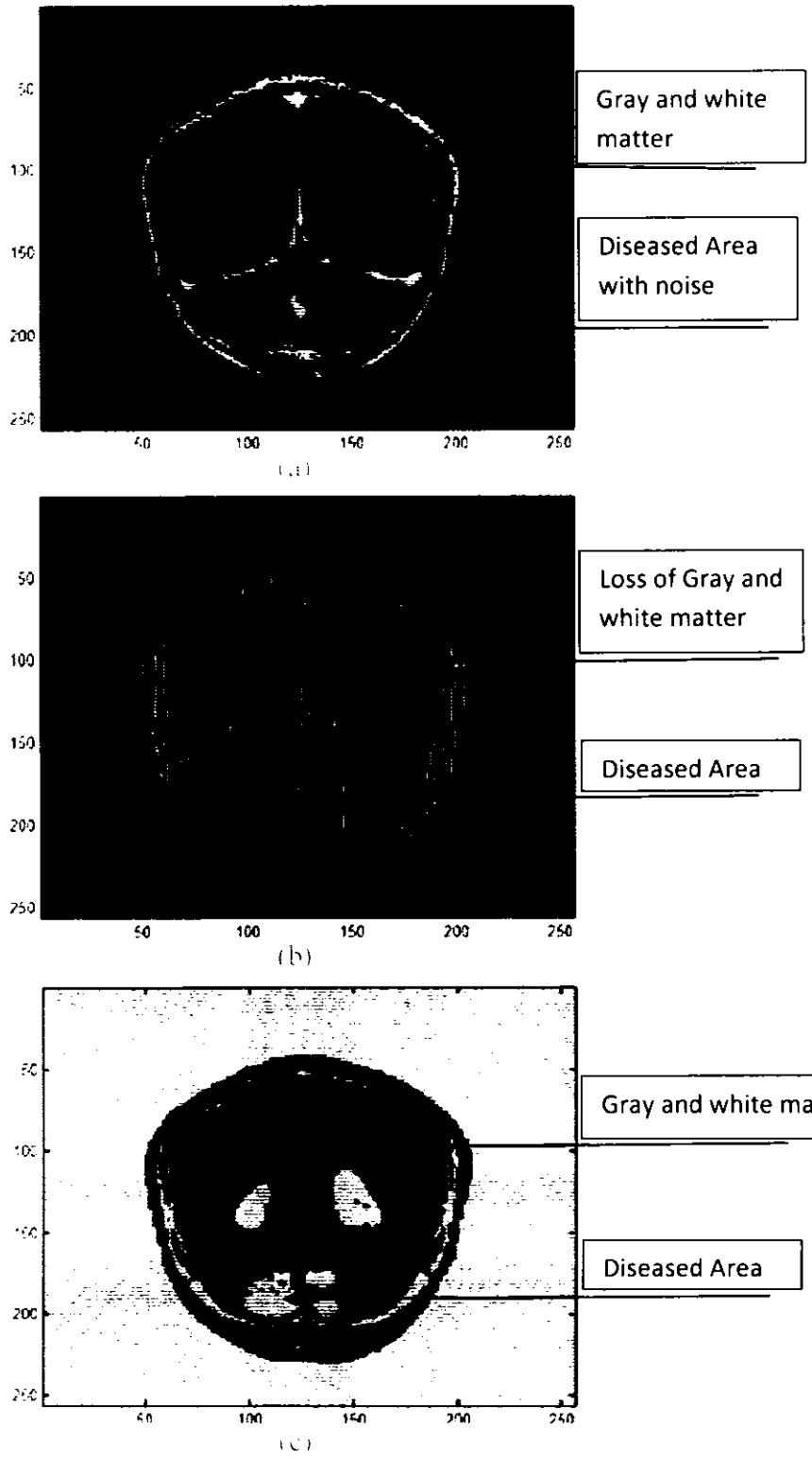

[illegible] case 2: (a) Simple K-means clustering [illegible] using squared Euclidean distance after applying DWPT [illegible] using cityblock distance after applying DWPT.

In this Figure 25 i increase the number of clusters from three to four, so K=4. This figure shows the results after K-means clustering. Figure 25 (a) shows the result of simple K-means clustering, on original MRI image. At this value of K it gives good information about the diseased area. Small errors appear near the diseased area as mentioned in Figure 25 (a). It also gives no information about the gray and white matter of the original image. Figure 25 (b) shows the result of my proposed technique using squared Euclidean distance function in K-means clustering at K=4. In this resultant image the area of the disease almost remains same and no errors appears near diseased area. The information of gray and white matter is missing. To get the information about the structure of gray and white matter i use cityblock distance function in K-means clustering for K=4. Figure 25 (c) shows the result of my proposed technique using cityblock distance function in K-means clustering. In this result the information of diseased area now becomes clear from noise. The additional information of gray and white matter appears individually and clearly. So the cityblock distance function gives good perform for four numbers of clusters.

Figure 26 shows patient 3, case 1

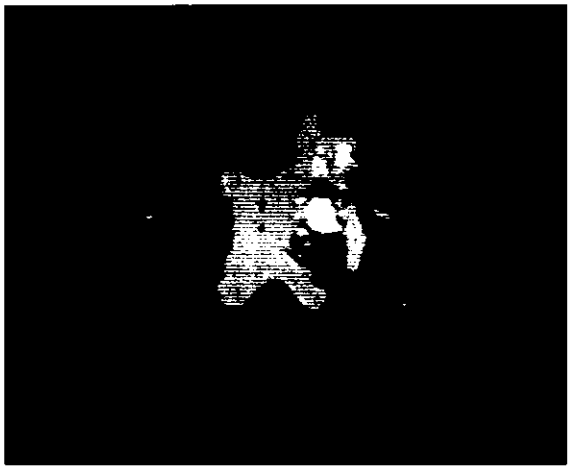

(a)

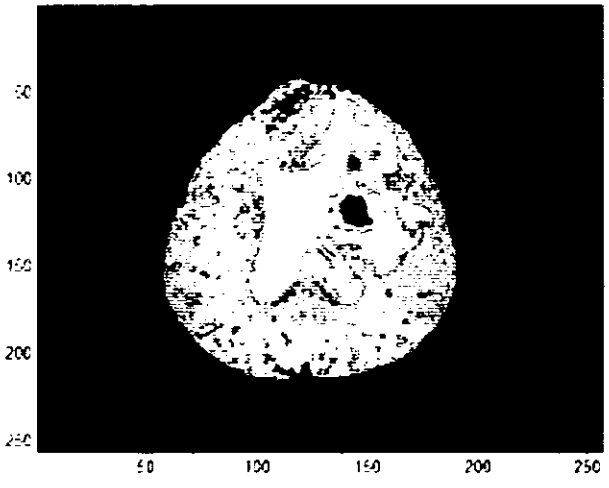

(b)

Figure 26: (a) Original gray scale image of patient 3, case 1 and (b) ... image with color map jet

Now the results of this patient for K=2, K=3 and K=4 are shows in Figure 27, Figure 28 and Figure 29 respectively.

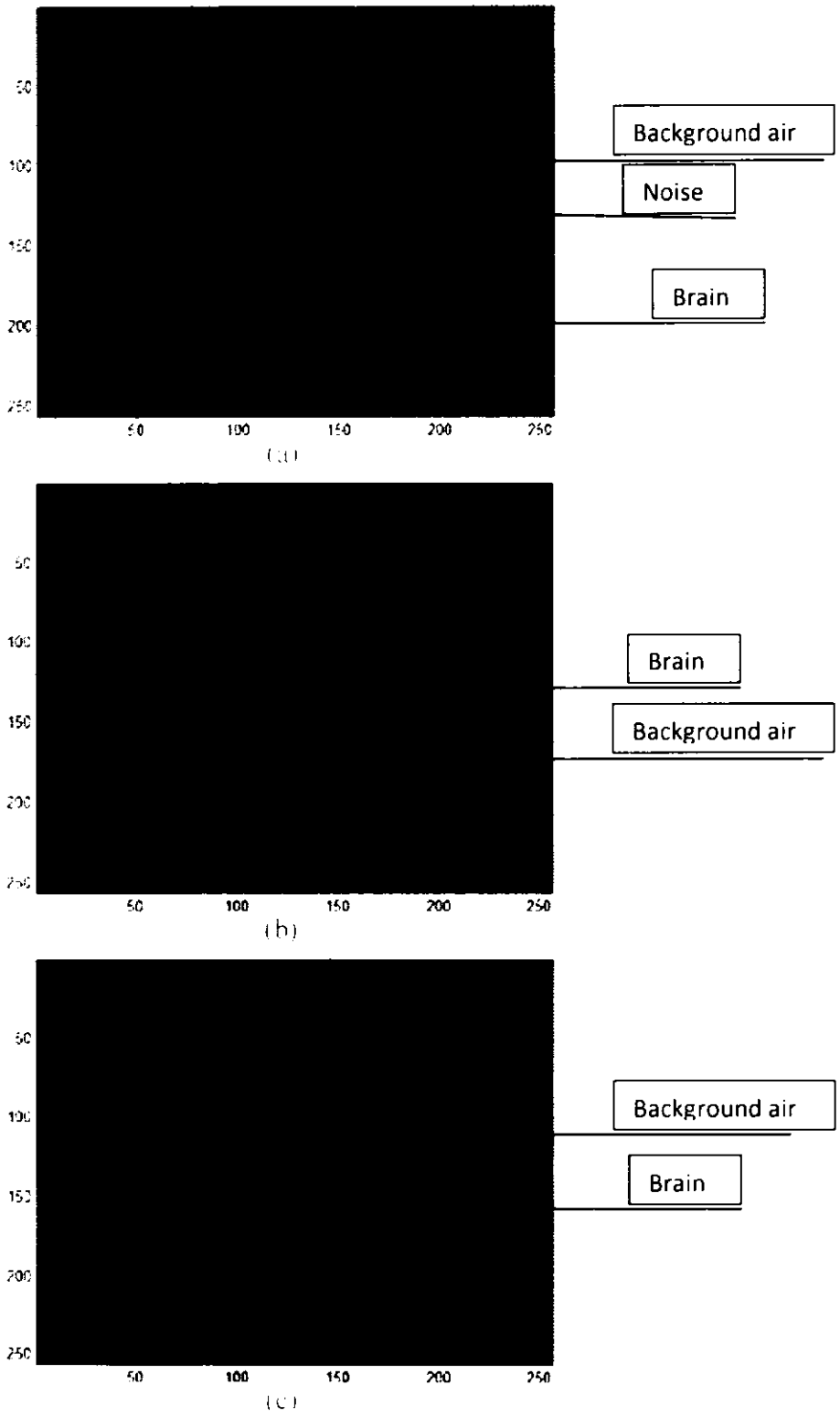

3. case 1: (a) Simple K-means clustering at K=3, (b) K-means
ed Euclidean distance after applying DWPT and (c) K-means
lock distance after applying DWPT

The Figure 27 shows the results after K-means clustering. In this Figure 27 i set the numbers of clusters as 2. Figure 27 (a) shows the result of simple K-means clustering, on original MRI image. It gives no information about the disease of the brain. It only segments the brain from the surrounding air. Here i can see one spot of error which is not required. Figure 27 (b) shows the result of my proposed technique using squared Euclidean distance function in K-means clustering. The result is improved because the noise disappears from the resultant image. Figure 27 (c) shows the result of my proposed technique using cityblock distance function in K-means clustering. It also segments the brain from surrounding air without introducing any noise. At this stage (K=2), the proposed technique is not providing better results. If i increase the number of clusters it will give better performance.

In Figure 28 i set the numbers of clusters as 3, so there will be three clusters in the resultant image. Figure 28 (a) shows the result of simple K-means clustering, on original MRI image. At this value of K it gives partial information of diseased area of brain. The noise in the air also appears. Figure 28 (b) shows the result of my proposed technique using squared Euclidean distance function in K-means clustering. The result is improved now because i have been able to mention ruff idea about the diseased area in the image. In this result the area of error also reduces. Figure 28 (c) shows the result of my proposed technique using cityblock distance function in K-means clustering. In this result the noise totally disappears and it also provide good information about the area of interest (disease).

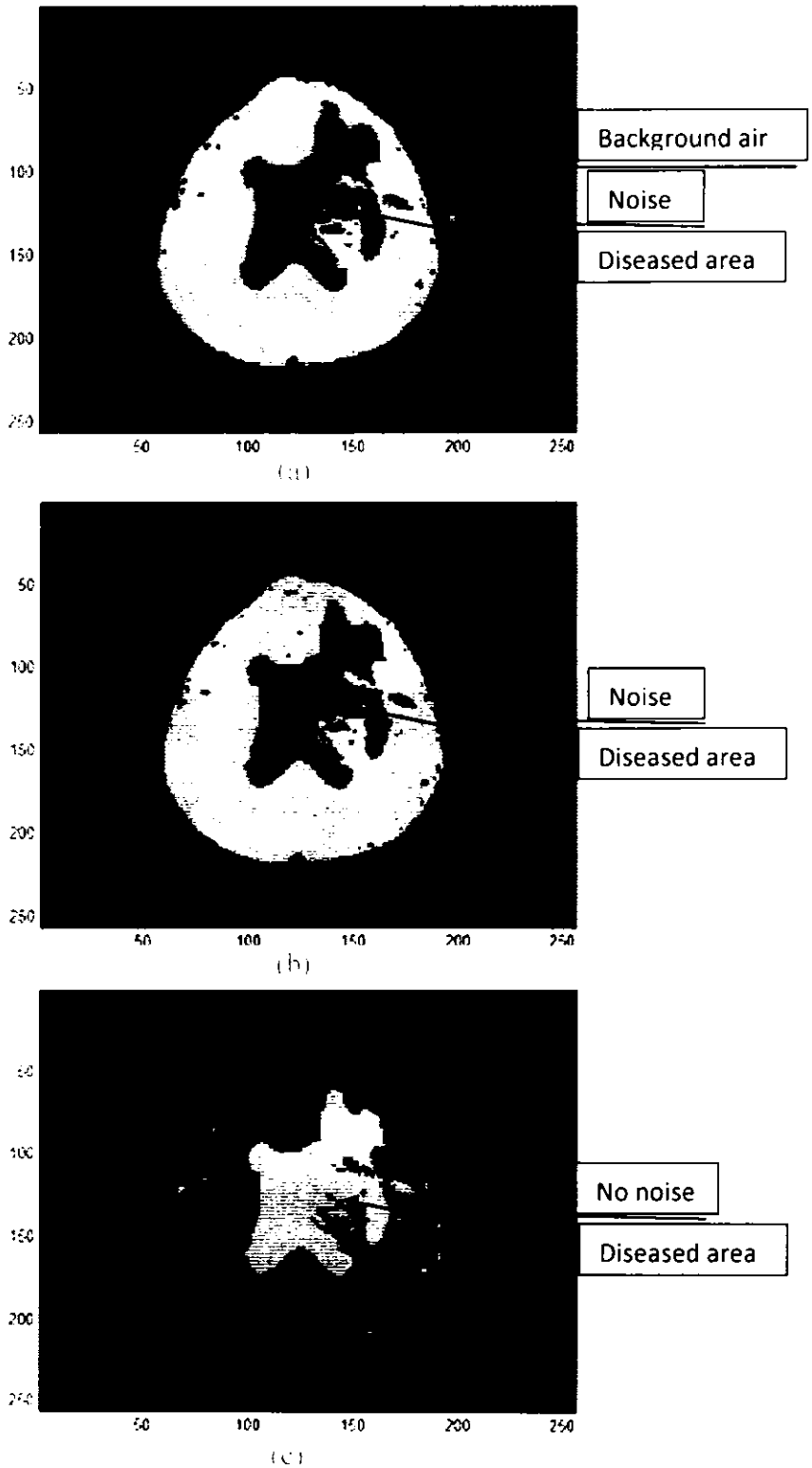

...squared Euclidean distance after applying DWPF ... cityblock distance after applying DWPF.

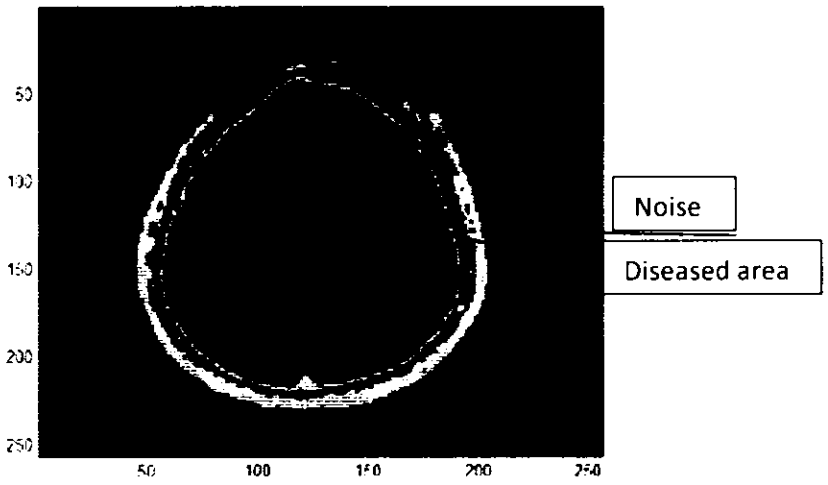

(a)

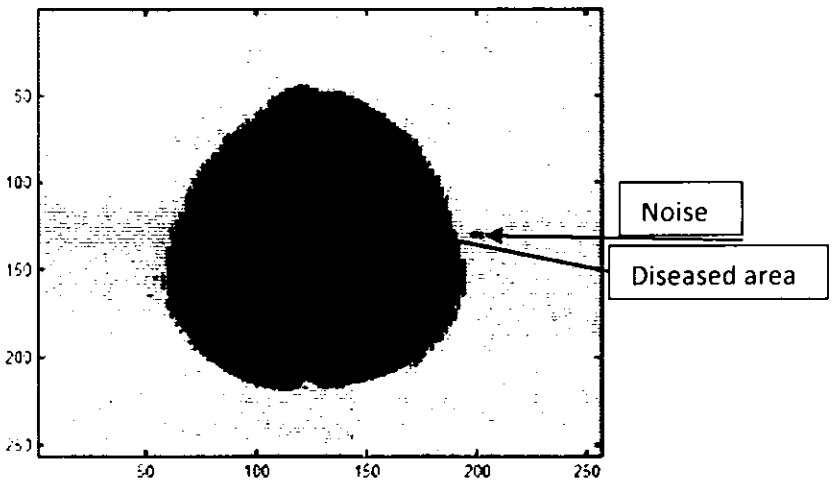

(b)

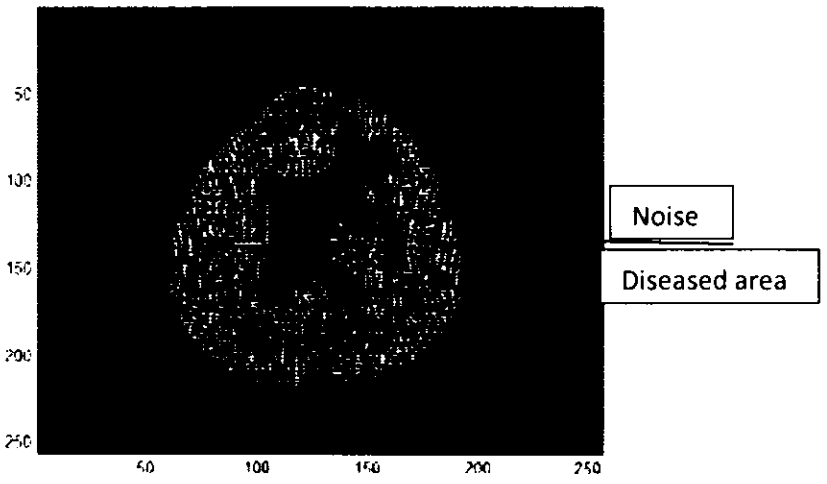

(c)

[illegible] Simple K-means clustering [illegible] squared Euclidean distance after applying DWPT [illegible] block distance after applying DWPT.

Figure 29 shows the results after K-means clustering. In this Figure 29 i set the value of K=4, so there will be four clusters in the resultant image. Figure 29 (a) shows the result of simple K-means clustering, on original MRI image. At this value of K it gives partial information of diseased area of brain. Figure 29 (b) shows the result of my proposed technique using squared Euclidean distance function in K-means clustering. The result is improved because i have been able to mention ruff idea about diseased area. Figure 29 (c) shows the result of my proposed technique using cityblock distance function in K-means clustering. In this case the noise appears in the surrounding of diseased area, which is not required.

Figure 30 shows patient 3, case 2

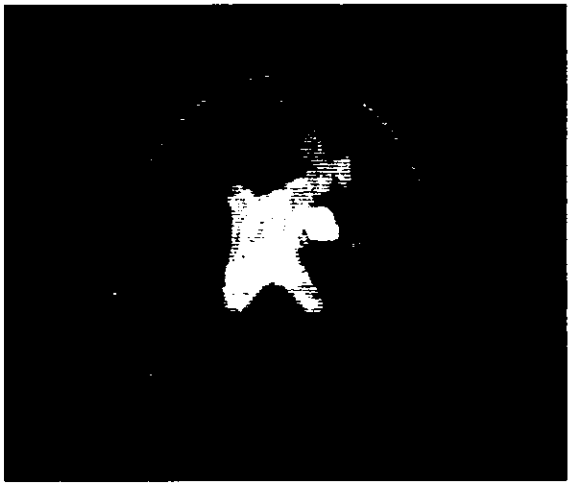

(a)

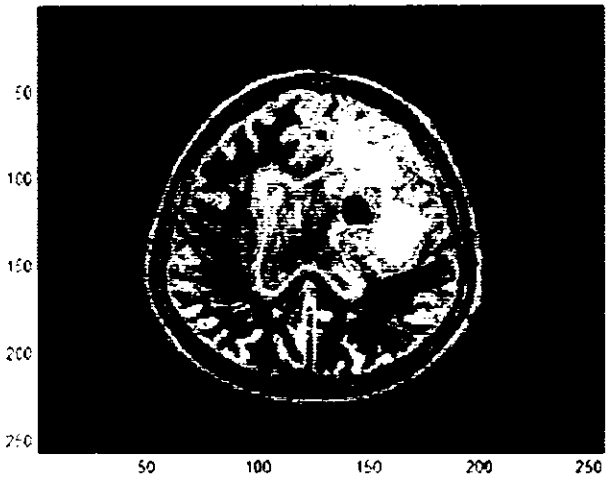

(b)

Figure 30: (a) Original gray scale image of patient 3, case 2 and (b) the same image with color map jet

Now the results of this patient for K=2, K=3 and K=4 are shows in Figure 31, Figure 32 and Figure 33 respectively.

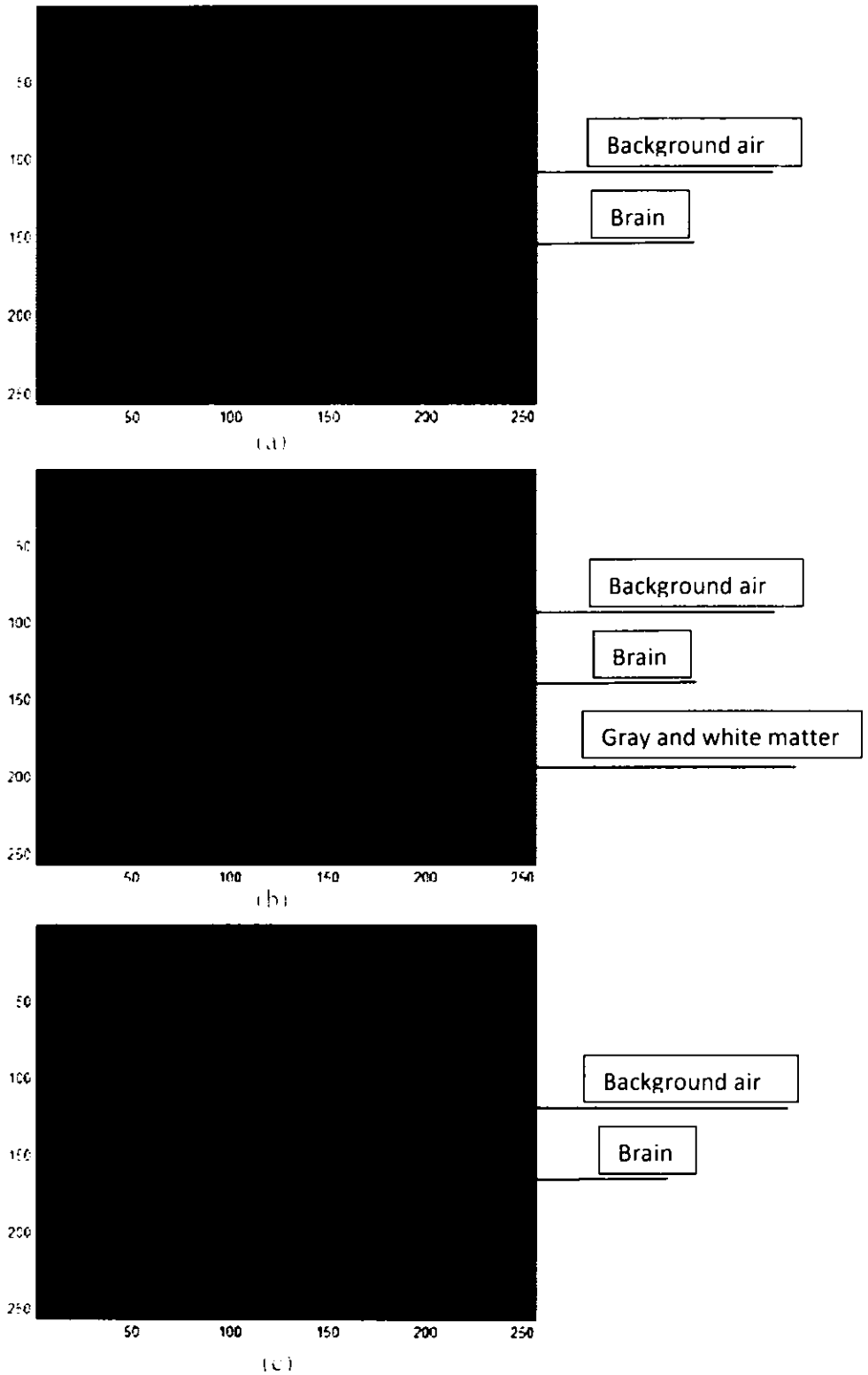

[illegible] case 2. (a) Simple K-means clustering at K = 2, (b) K-means [illegible] ed Euclidean distance after applying DWPF and (c) K-means [illegible] ock distance after applying DWPF.

Figure 31 shows the results after K-means clustering. In this Figure 31 i set the numbers of clusters as 2. Figure 31 (a) shows the result of simple K-means clustering, on original MRI image. It gives no information about the disease of the brain. So i have not been able to segment the disease. It only segments the brain from the surrounding air. Figure 31 (b) shows the result of my proposed technique using squared Euclidean distance function in K-means clustering. The result is improved because some information about the diseased area appears along with some gray and white matter information. Figure 31(c) shows the result of my proposed technique using cityblock distance function in K-means clustering. It also only segments the brain area from the surrounding air.

In Figure 32 i set the value of K=3, so there will be three clusters in the resultant image. Figure 32 (a) shows the result of simple K-means clustering, on original MRI image. At this value of K it gives partial information of diseased area of brain. Figure32 (b) shows the result of my proposed technique using squared Euclidean distance function in K-means clustering. The result is improved because some boundaries of diseased area become sharp. Figure 32 (c) shows the result of my proposed technique using cityblock distance function in K-means clustering. In this result the noise totally disappears and it also provide good information about the area of interest (disease). It still gives no information about the gray and white matter of brain. If i increase the number of clusters it will give better performance.

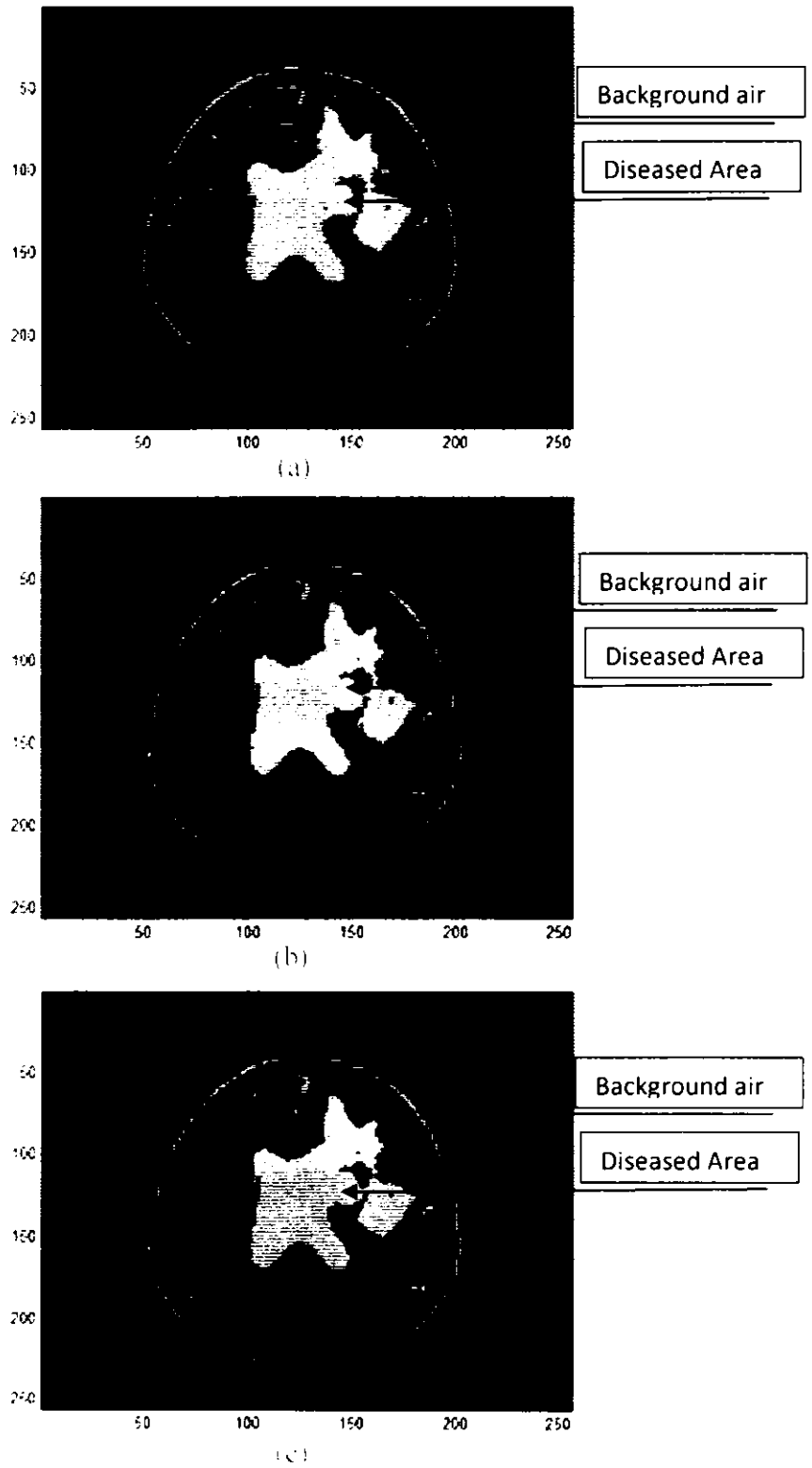

[illegible] Case 2: (a) Simple K-means clustering after [illegible] using squared Euclidean distance after applying DWPT (b) K-means clustering using cityblock distance after applying DWPT

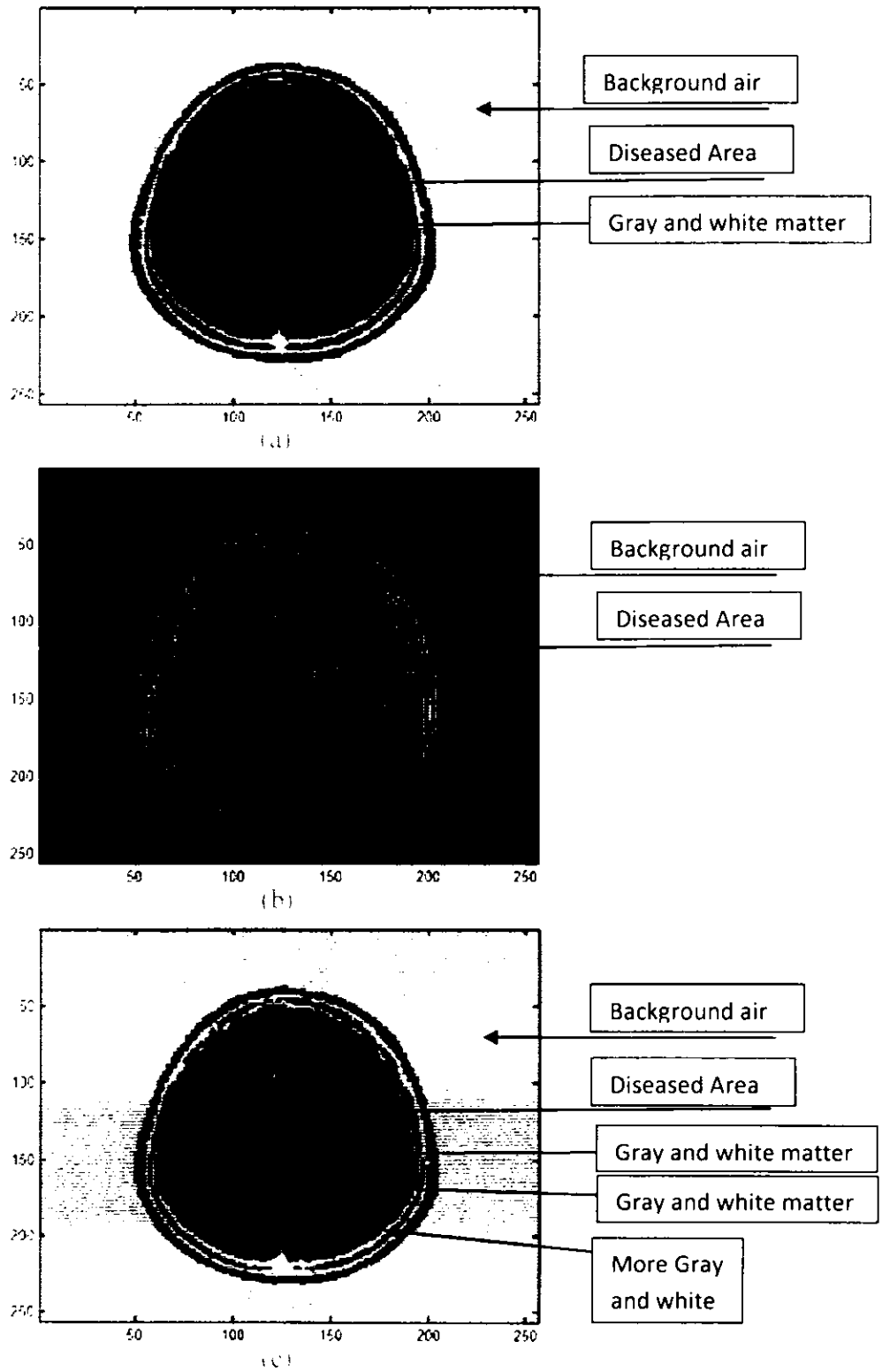

Case 2: (a) Simple K-means clustering (b) K-
ed Euclidean distance after applying DWPT and (c) K-
ock distance after applying DWPT.

In this Figure 33 i increase the number of clusters from three to four, so K=4. This figure shows the results after K-means clustering. Figure 33 (a) shows the result of simple K-means clustering, on original MRI image. At this value of K it gives good information about the diseased area. It also gives some information about the gray and white matter of the original image. Figure 33 (b) shows the result of my proposed technique using squared Euclidean distance function in K-means clustering at K=4. In this resultant image the area of the disease almost remains same. The information of gray and white matter is missing. To get the information about the structure of gray and white matter i use cityblock distance function in K-means clustering for K=4. Figure 33 (c) shows the result of my proposed technique using cityblock distance function in K-means clustering. In this result the information of diseased area becomes clear from noise. The additional information of gray and white matter appears individually and clearly. The boundary of the diseased area also appears. So the cityblock distance function gives good perform for four numbers of clusters.

All the above result shows that the proposed technique performs better using cityblock distance in K-means clustering when i set the numbers of clusters as 4. The results of Figure (13, 25 and 33) clearly justify that the cityblock distance function gives better performance as compare to squared Euclidean distance function in K-means clustering. The result of patient 2, case 1 is an example where difference is also clear. The results are shown in Figure 34 as:

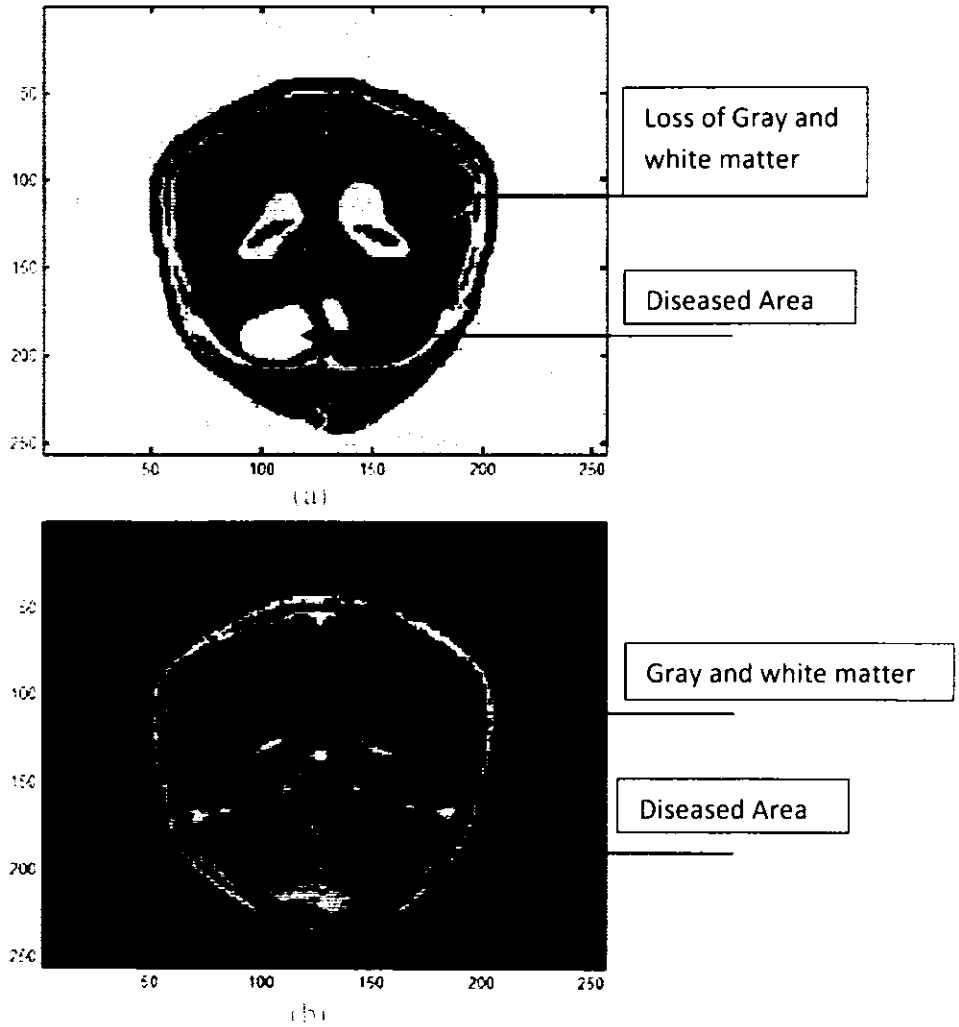

[illegible] K-means clustering using squared [illegible] using DWPT for K=4 and (b) K-means clustering using city block [illegible] using DWPT for K=4

There are some results where cityblock distance function is not performing better as shown in Figure (12, 17, 29 and 31). The proposed technique using cityblock distance function in K-means clustering is not performing better mostly when i set the value of K=2 or K=3. Example of K=2 is shown in Figure 35 as:

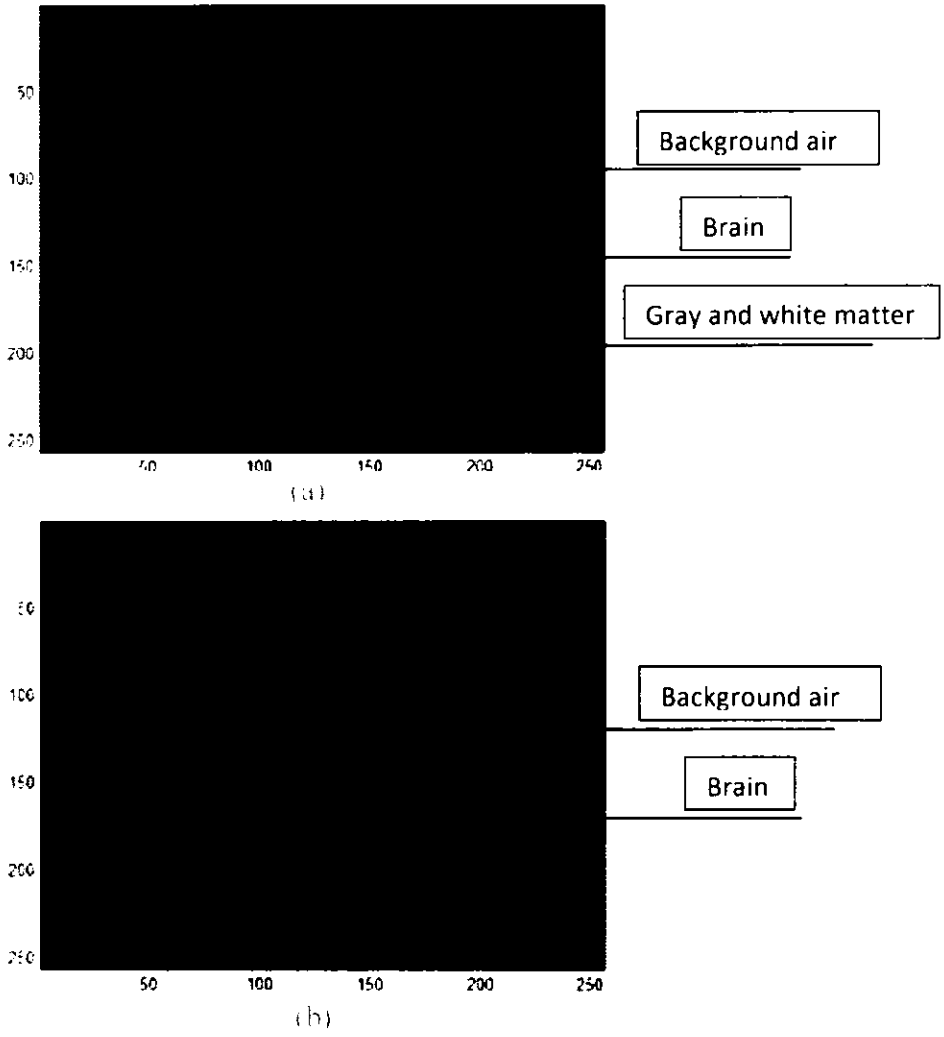

Figure 35. For patient 3, case 2 at K=2 (a) K-means clustering using squared Euclidean distance after applying DWPF and (b) K-means clustering using cityblock distance after applying DWPF

For more detail see the results of Figure (12, 17 and 29).

CHAPTER # 5

CONCLUSION

5.1. Conclusion

Proposed segmentation technique is an application of medical image segmentation technique for assisting in diagnosis of human brain diseases. Designed technique is very efficient in its performance and has the flexibility to adjust the parameters easily according to the individual case requirement. As discussed in Chapter 4, the results of simple K-means clustering are improved significantly by applying proposed Discrete Wavelet Packet Frames (DWPF) before K-means clustering i.e. using selected DWPFs for application of K-means clustering. Normally clustering of Magnetic Resonance Imaging (MRI) images of human brain is based upon intensity values. After applying proposed DWPF, the results of K-means clustering become better and better visualization of the diseased area is obtained. Clustering is performed by using two different distances. The K-mean clustering results using cityblock distance provide more information whereas the K-means clustering results of squared Euclidean distance only gives better information about the diseased area in spite of other detailed structural information of gray and white matter of human brain.

5.2. Future Extensions of Work

There are two possibilities for the extension of work presented in this thesis in the following two main areas.

- Selection of Wavelet Packet Frames (WPFs)

- Extension of K-means

5.2.1. Selection of WPFs

In the proposed technique the WPFs are selected on the bases of energy and entropy value arrangement as discussed in 3.5. The results may be improve by using any other selection criteria for useful WPFs i.e. pre clustering or learning mechanism.

5.2.2. Extension of K-means

K-mean can only converge to local minimum, even though the recent research has shown with large probability K-means could converge to the global optimum only when clusters are well separated [4. 5]. The algorithm of K-means has been extended in many other ways. Some of them deal with supplementary commonsense rules intended to increase the probability of solving problem, involving the minimum cluster size and splitting and merging clusters. Two well known modifications of K-means in pattern recognition are ISODATA [54] and FORGY [55]. In simple K-means clustering one data point is a member of single cluster. In 1973 Dunn propose fuzzy c-means clustering [56] which is later improved by Bezdek [57] is an extension of simple K-means clustering where one data point can be a part of multiple clusters. In K-mediod the clusters are represented by using the median of data in spite of mean [58]. Using the above mentioned techniques results of MRI segmentation may be improved.

5.3. Main contribution

I am using Discrete Wavelet Packet Frames (DWPF) before applying K-means clustering. In the history of image segmentation or clustering DWPF has not been used with K-means clustering. So it the first time i am using DWPF in K-means clustering as preprocessing step for segmentation and my results show that the segmentation is improved greatly using DWPFs.

References:

[1]. D.L. Pham, C. Xu and J.L. Prince, "A Survey of Current Methods in Medical Image Segmentation", annual review of Biomedical engineering, vol. 2, pp. 315-337, 2000.

[2]. S. Nassir, "Image Segmentation Based on Watershed and Edge Detection Techniques", International Arab Journal of Information Technology, Vol. 3, April, 2006.

[3]. H.P. Ng, S.H. Ong, K.W.C. Foong, P.S. Goh and W.L. Nowinski," Medical image segmentation using K-means clustering and improved watershed algorithm", image analysis and interpretation, IEEE Southwest Symposium, pp. 61-65, 2006.

[4]. M. Meila, "The uniqueness of a good optimum for k-means", Proceedings of the 23rd International Conference on Machine Learning, pp. 625–632, 2006.

[5]. A.K. Jain," Data Clustering: 50 Years Beyond K-Means", Pattern Recognition Letters, vol. 13, pp. 651-666, 2009.

[6]. S.S. Al-amri, N.V. Kalyankar and S.D. Khamitkar, "Image segmentation by using edge detection", International Journal on Computer Science and Engineering, vol. 2, pp. 804-807, 2010.

[7]. H. Tang, E.X. Wu, Q.Y. Ma, D. Gallagher, G.M. Perera, and T. Zhuang, "MRI Brain Image Segmentation by Multi-Resolution Edge Detection and Region Selection," Computerized Medical Imaging and Graphics, vol. 24, no. 6, pp. 349-357, 2000.

[8]. M.M. Ahmed and D.B. Mohammad, "Segmentation of Brain MR Images for Tumor Extraction by Combining Kmeans Clustering and Perona-Malik Anisotropic Diffusion Model," International Journal of Image Processing, vol. 2, pp. 27, 2008.

[9]. http://en.wikipedia.org/wiki/MRI_contrast_agent

[10]. M. Unser and A. Akram, "A review of wavelets in biomedical applications", proceedings of the IEEE, vol. 84, no. 4, April 1996.

[11]. R. Polikar, "The story of wavelets", Physics and modern topics in mechanical and electrical engineering, pp. 192-197, 1999.

[12]. P.M. Mahajan, S.R. Kolhe and P.M. Patel, "A review of automatic fabric defect detection techniques," advances in computational research, vol. 1, pp. 18-29, 2009.

[13]. X. Xie, "A review of recent advances in surface defect detection using texture analysis techniques," jurnal Elcvia, vol. 7, 2008.

[14]. L.P. Clarke, R.P. Velthuizen, S. Phuphanich, J.D. Schellenberg, J.A. Arrington, and M. Silbiger, "MRI: stability of three supervised segmentation techniques", Mag. Res. Imag., vol. 11, pp. 95–106, 1993.

[15]. M. Vaidyanathan, L.P. Clarke, R.P. Velthuizen, S. Phuphanich, A.M. Bensaid, et al., "Comparison of supervised MRI segmentation methods for tumor volume determination during therapy", Mag. Res. Imag., vol. 13, pp. 719–728, 1995.

[16]. L.O. Hall, A.M. Bensaid, L.P. Clarke, R.P. Velthuizen, M.S. Silbiger, and J.C. Bezdek, "A comparison of neural network and fuzzy clustering techniques in segmenting magnetic resonance images of the brain", IEEE T. Neural Networks, vol. 3, pp. 672–682, 1992.

[17]. M. Joliot and B.M. Mazoyer, "Three-dimensional segmentation and interpolation of magnetic resonance brain images", IEEE T. Medical Imaging, vol. 12, pp. 269–277, 1993.

[18]. J.L. Prince, Q. Tan, and D. Pham, "Optimization of MR pulse sequences for Bayesian image segmentation", Medical Physics, vol. 22, pp. 1651–1656, 1995.

[19]. D.L. Pham, J.L. Prince, A.P. Dagher, and C. Xu, "An automated technique for statistical characterization of brain tissues in magnetic resonance imaging", Int. J. Patt. Rec. Art. Intel., vol. 11, pp. 1189-1211, 1997.

[20]. R. Momenan, D. Hommer, R. Rawlings, U. Rutimann, M. Kerich, and D. Rio, "Intensity-adaptive segmentation of single-echo T1-weighted magnetic resonance images", Human Brain Mapping, vol. 5, pp. 194–205, 1997.

[21]. K.H. Hohne and W.A. Hanson, "Interactive 3-D segmentation of MRI and CT volumes using morphological operations", J. Comp. Assist. Tom., vol. 16, pp. 285–294, 1992.

[22]. W. Menhardt and K.H. Schmidt, " Computer vision on magnetic resonance images", Pattern recognition lettters, vol. 8, pp. 73–85, 1988.

[23]. J.C. Rajapakse, J.N. Giedd, and J.L. Rapoport, "Statistical approach to segmentation of single-channel cerebral MR images", IEEE T. Med. Imag., vol. 16, pp. 176–186, 1997.

[24]. Y. Wang, T. Adah, S. Kung ad and Z. Szabo, "Quantification and segmentation of brain tissues from MR images", Nneural network approach IEEE T. Image Processing, vol. 7, pp. 1165–1181, 1998.

[25]. M.W. Vannier, R.L. Butterfield, D. Jordan, W.A. Murphy, R.G. Levitt and M. Gado, "Multispectral analysis of magnetic resonance images", Radiology, vol. 154, pp. 221–224, 1985.

[26]. K.O. Lim and A. Pfefferbaum, "Segmentation of MR brain images into cerebrospinal fluid and white and gray matter", J. Comp. Assist. Tom., vol. 13, pp. 588–593, 1989.

[27]. H.S. Choi, D.R. Hanynor, and Y. Kim, "Partial volume tissue classification of multichannel magnetic resonance images a mixel model", IEEE T. Med. Imag, vol. 10, pp. 395–407, 1991.

[28]. M.I. Kohn, N.K. Tanna, G.T. Herman, S.M. Resnick, et al. "Analysis of brain and cerebrospinal fluid volumes with MR imaging", Radiology, vol. 178, pp. 115–122, 1991.

[29]. G. Gerig, J. Martin, R. Kikinis, O. Kubler, M. Shenton, and F.A. Jolesz, " Unsupervised tissue type segmentation of 3D dual-echo MR head data", Image and Vision Computing, vol. 29, pp. 100–132, 1985.

[30]. Z. Liang, J.R. MacFall, and D.P. Harrington, "Parameter estimation and tissue segmentation from multispectral MR images", IEEE T. Med. Imag., vol. 13, pp. 441–449, 1994.

[31]. G.J. Harris, P.E. Barta, L.W. Peng, et al. "MR volume segmentation of gray matter and white matter using manual thresholding: dependence on image brightness," American journal of neuroradiology, vol. 15, pp. 225–230, 1994.

[32]. J. Kaufhold, M. Schneider, A.S. Willsky, and W.C. Karl, "A statistical method for efficient segmentation of MR imagery," Int. J. Patt. Rec. Art. Intel., vol. 11, pp. 1213–1231, 1997.

[33]. C. Tsai, B.S. Manjunath, and R. Jagadeesan, "Automated segmentation of brain MR images," Patt.Rec., vol. 28, pp. 1825–1837, 1995.

[34]. W.E. Reddick, J.O. Glass, E.N. Cook, T.D. Elkin, and R.J. Deaton, "Automated segmentation and classification of multispectral magnetic resonance images of brain using artificail neural networks," IEEE T. Med. Imag., vol. 16, pp. 911–918, 1997.

[35]. A. Simmons, P.S. Tofts, G.J. Barker and S.R. Arridge, "Sources of intensity nonuniformity in spin echo images at 1.5T," Mag. Res. Med., vol. 32, pp. 121–128, 1994.

[36]. B.R. Condon, J. Patterson, D. Wyper, A. Jenkins and D.M. Wadly, "Image non-uniformity in magnetic resonance imaging: its magnitude and methods for its correction", The British Journal of Radiology, vol. 60, pp. 83–87, 1989.

[37]. J.G. Sled and G.B. Pike, "Standing-wave and RF penetration artifacts caused by elliptic geometry," Medical Imaging, IEEE Transactions, vol.17, pp. 653–662, 1998.

[38]. W.J. Carper, T.W. Lilesand, and R.W. Kieffer, "The use of Intensity-Hue-Saturation transformation for merging SPOT panchromatic and multispectral image data", Photogrammetric Engineering and Remote Sensing, pp. 459–467, 1990.

[39]. P.S. Chavez, S.C. Sildes, and J.A. Anderson, "Comparison of three different methods to merge multiresolution and multi-spectral data: Landsat TM and SPOT panchromatic", Photo- grammetric Engineering and Remote Sensing, pp. 295–303, 1991.

[40]. H. Li, B.S. Manjunath, S.K. Mitra, "Multisensor image fusion using the wavelet transform", Graphical Models and Image Processing, pp. 235–245, 1995.

[41]. W.J. Carper, T.W. Lilesand, and R.W. Kieffer, "The use of Intensity-Hue-Saturation transformation for merging SPOT panchromatic and multispectral image data," Photogrammetric Engineering and Remote Sensing, vol.56, pp. 459–467, 1990.

[42]. Li S. T, Ianes T. K and Wang Y. N.," Using the discrete wavelet frame transform to merge Landsat TM and SPOT panchromatic images". Information Fusion, vol. 3, pp. 17-23, Mar. 2002.

[43]. P.W. Hamilton, P.H. Bartels, D. Thompson, N.H. Anderson, R. Montironi and J.M. Sloan, "Automated location of dysplastic fields in colorectal histology using image texture analysis," The Journal of pathology, vol. 182, pp. 68-75, 1997.

[44]. A.N. Esgiar, R.N.G. Naguib, B.S. Sharif, M.K. Bennett and A. Murray, "Microscopic image analysis for quantitative measurement and feature identification of normal and cancerous colonic mucosa," Information Technology in Biomedicine, IEEE Transactions vol. 2, pp 197-203, 1998.

[45]. F. Gilles, A. Gentile, V.L.Doussal, F. Bertrand and E. Kahn, "Grading of cystosarcoma phyllodes by texture analysis of tissue architecture," Anal. Quant. Cytol. Histol., vol. 16, pp. 95-100, 1994.

[46]. T. Irinopoulou, J. Rigaut, M. Benson, "Toward objective prognostic grading of prostatic carcinoma using image analysis," Anal. Quant. Cytol. Histol., vol. 15, pp. 341-344, 1993.

[47]. V. Musoko, "Biomedical signal and processing", PhD thesis, Institute of Chemical Technology, Prague Department of Computing and Control Engineering, 2005.

[48]. 2011 (February). Google scholar. http://scholar.google.com.

[49]. A. Raza, G. Usman and S. Asim, "Data clustering and its applications", http://members.tripod.com/asim_saeed/paper.htm

[50]. http://www.norusis.com/pdf/SPC_v13.pdf (online part of a book).

[51]. http://stn.spotfire.com/spotfire_client_help/hc/hc_city_block_distance.htm

[52]. H.S. Thomsen, S.K. Morcos and P. Dawson,"Is there a causal relation between the administration of gadolinium-based contrast media and the development of nephrogenic systemic fibrosis (NSF)?", Clinical Radiology 61, November 2006.

[53]. C. Junchul and S. George," Subband Image Segmentation Using VQ for Content-Based Image Retrieval", pp. 486 - 488, 2001.

[54]. G.H. Ball and D.J. Hall, "ISODATA, a novel method of data analysis and pattern classification", Tech. rept. NTIS AD 699616, Stanford Research Institute, Stanford, CA, 1965.

[55]. E.W. Forgy, "Cluster analysis of multivariate data: efficiency vs interpretability of classifications", Biometrics, vol. 21, pp. 768–769, 1965.

[56]. J. C. Dunn, "A fuzzy relative of the ISODATA process and its use in detecting compact well-separated clusters", Journal of Cybernetics, 3, pp. 32–57, 1973.

[57]. J.C. Bezdek, " Pattern recognition with fuzzy objective function algorithms", Plenum Press, 1981.

[58]. L. Kaufman and P.J. Rousseeuw, "Finding groups in data: An introduction to cluster analysis", Wiley series in Probability and Statistics, 2005.